Pergamon

*Prog. Polym. Sci.*, Vol. 22, 829–871, 1997

0079–6700/97 $32.00

**PPI: S0079–6700(97)00008–7**

# THE APPLICATION OF SIDE-CHAIN LIQUID-CRYSTALLINE POLYMERS

**CHAIN-SHU HSU**

*Department of Applied Chemistry, National Chiao Tung University, Hsinchu, Taiwan, Republic of China*

## CONTENTS

## 1. INTRODUCTION

Side-chain liquid-crystalline polymers (LCPs), which represent a combination of liquid-crystalline behavior and polymeric properties, have been the subject of intensive research during the last decade. Systematic investigation of the synthesis of side-chain LCPs began only after Ringsdorf and co-worker proposed that a flexible spacer should be inserted between the polymeric backbones and mesogenic side groups to decouple the motions of the backbone and side groups in the liquid-crystalline state. On the basis of the spacer model, a large number of side-chain LCPs containing rod-like or disk-like mesogens were synthesized. Different smectic, chiral smectic, nematic and cholesteric mesophases are exhibited by these polymers that are based on different mesogenic groups and polymer backbones. Much information concerning the properties of side-chain LCPs under the influence of an external electric or magnetic field is also well documented. This field has been highly developed because of the potential applications of side-chain LCPs. So far, various potential applications have been considered for the side-chain LCPs. Broadly speaking, applications fall into the following fields: optical data storage, non-linear optics, stationary phases for gas chromatography, supercritical-fluid chromatography and high-performance liquid chromatography, solid polymer electrolytes, separation membranes and display materials.

Most of these fields were reviewed in 1989.[1] Therefore, we shall discuss only the recent progress in the applications of side-chain LCPs, in most of the cases based on the literature published since 1989.

## 2. APPLICATION OF SIDE-CHAIN LCPS IN OPTICAL DATA STORAGE

The first example of a side-chain LCP as a reversible optical data storage material was demonstrated by Shibaev *et al.* in 1983.[2] The advantages of side-chain LCPs over low-molar-mass liquid crystals as image storage materials are as follows. (1) Because of the glass transition phenomenon ($T_g$), segmental motion of the polymer chains can be frozen-in; thus it is expected that the stored image can be kept stable below $T_g$ for a long time. (2) Good film-forming properties of the polymers allow cell-free performance of the image storage materials, which is evidently favorable from the applicational viewpoint. (3) Low fluidity of the polymers is favorable for the long-term stability of the stored image.

The study of side-chain LCPs in optical data storage was at an early stage when McArdle reviewed this field in 1989.[1] Since then, a large number of side-chain LCPs to be used for optical data storage, have been reported in the literatures. Broadly speaking, the applications of side-chain LCPs in optical data storage fall into two classes: heat-mode recording and photo-mode recording. Shibaev *et al.*[2] and Coles and Simon[3] reported the laser-addressed side-chain LCPs in heat-mode recording. McArdle reviewed most of this kind of heat-mode recording. Photo-mode recording was first reported by Wendorff *et al.* as "holographic" optical storage in 1987.[4] In their system, composed of LCPs with side-chain photochromic azobenzene moieties, photoirradiation caused isomerization of the photochromic molecules, inducing "grating" in the LCP. The grating is produced by the change in the refractive index of the medium resulting from isomerization. The advantage of photo-mode recording over heat-mode recording lies in the superior resolution, fast writing speed and the possibility of multiplex recording in photo-mode recording. It is not intended to review all side-chain LCPs

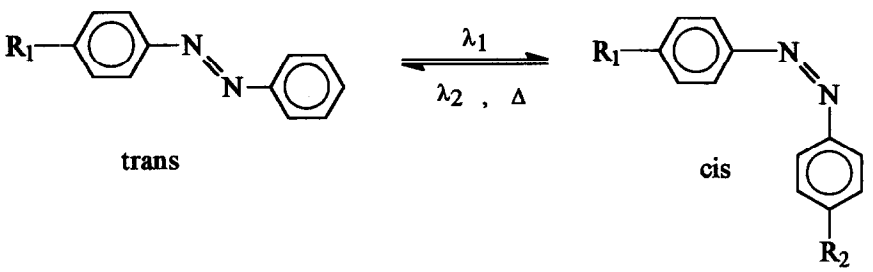


Fig. 1. *Cis–trans* isomerization of substituted azobenzene compounds.

for optical data storage here; rather, some representative examples of photo-mode recording are briefly discussed.

### 2.1. *Side-chain LCPs containing azobenzene chromophores as reversible optical data storage materials*

It is well known that the azobenzene group can exist in two configurations: the *trans* or *E* form and the *cis* or *Z* form, as illustrated in Fig. 1. By irradiating with light of wavelength $\lambda_1$ and $\lambda_2$, the geometric configuration of the azo bond in azobenzene-based compounds can be reversibly switched from *trans* to *cis*. However, the *cis* state is thermodynamically unstable with respect to the *trans* state; therefore a thermal relaxation process occurs in the dark state, denoted in Fig. 1 as Δ.

Since Wendorff *et al.* first demonstrated reversible optical data storage properties in the azobenzene-containing side-chain LCP films in 1987[4] there has been a lot of interest in this area.[5–15] A homopolymer containing a *p*-nitroazobenzene bound as side chain in a polyester through an oxygen atom and a spacer of six methylene units was used in Wendorff's study (Fig. 2).

The writing process consists, in a first step, of orientation of the liquid-crystalline film by an external field, followed by irradiation with polarized laser light in the liquid-crystalline state or in the glassy state. This involves optically inducing a *trans–cis* conformational transition in the mesogenic side chains. The photogenerated *cis* form, owing to its non-mesogenic character, leads to a local change in the orientation distribution of the

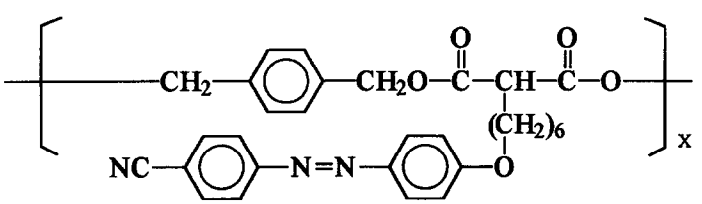


LCP-1 g 43 $S_A$ 94 n 104 i

Fig. 2. The chemical structure of liquid-crystalline polyesters (LCP-1) containing azobenzene side groups, with transitions glassy to smectic A, nematic and isotropic as indicated (in °C).[4]

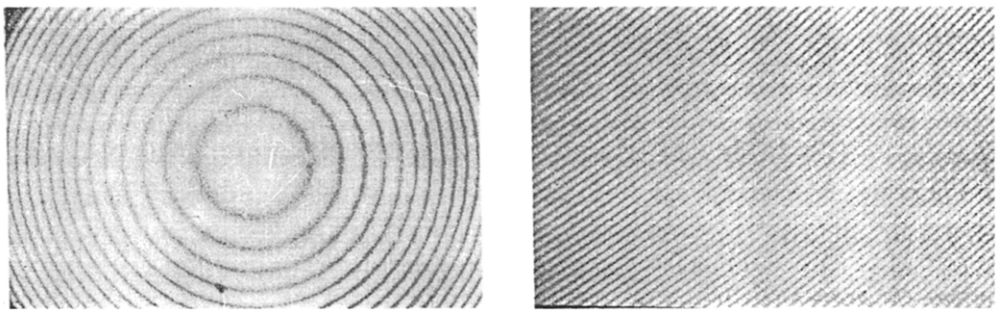

(A) (B)

Fig. 3. Center (A) and outer region (B) of Fresnel zone phase plate, stored by holographic techniques in a 7 $\mu$m film of the liquid-crystalline side-chain polymer LCP-1.

liquid-crystalline matrix when the polymer is simultaneously heated locally. The perturbation generated in this way is much greater than it would be in an amorphous matrix. After the light is switched off, the perturbation is frozen-in and is retained, even if the azobenzene relaxes back to its *trans* form (see Fig. 3). To erase the stored information, the side-chain LCP is heated to a temperature above the clearing temperature, $T_{NI}$, thereby orienting.

Side-chain LC copolymers with both photosensitive (azobenzene) and non-photosensitive side groups were also used in these studies.[16–26] Copolymers of the structure shown in Fig. 4 were used by Anderle *et al.*[16] After irradiation by the polarized laser light, reorientation of the azobenzene moieties actually affects the neighboring non-photosensitive mesogenic groups, either below or above the glass transition temperature. This is due to the cooperative motion of the neighboring groups.

All these liquid-crystalline azobenzene-containing polymers have their glass transition temperature slightly higher than room temperature because of the requirement of flexibility

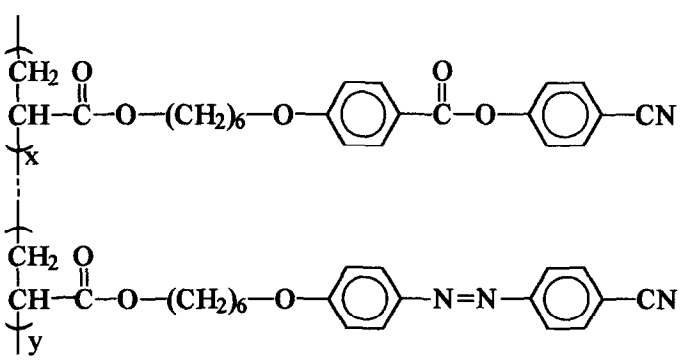


Fig. 4. Chemical structure of liquid-crystalline polyacrylates containing 4-cyanophenylbenzoate and 4-cyanophenylazobenzene side groups.[16]

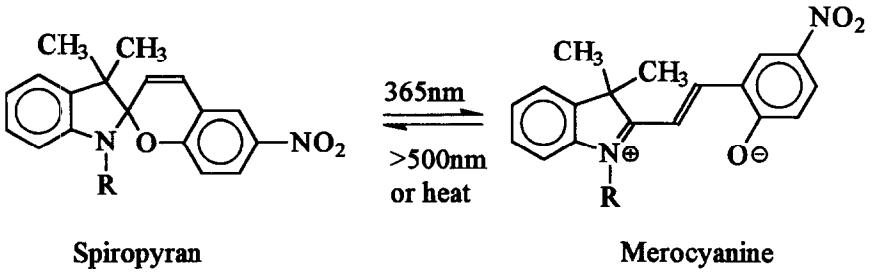


Fig. 5. Photochromic reaction of the spiropyran chromophores.

so as to form a mesophase. In principle, the higher the glass transition temperature of the polymer, the greater the stability of the writing at room temperature when this is well below the glass transition temperature.

Some amorphous azo polymers with high glass transition temperature have been synthesized and tested recently for reversible optical storage processes.[27–30] High glass transition temperatures are obtained by using very short or no spacers between the main chain and the azo side groups. This results in a significant increase in the stability of the written material. It has thus been proved that liquid crystallinity is not a necessary condition for a material to exhibit reversible optical storage properties. Writing by using polarized laser light with wavelength equal to that of the absorbance of the azo group can be performed at room temperature in the glassy state. The birefringence can be monitored with a light beam whose wavelength is out of the region of absorbance of the azo polymer. The written information can be erased either by heating the polymer above its glass transition temperature or by irradiating with circularly polarized light.

### 2.2. *Side-chain LCPs containing spiropyran chromophores as reversible optical data storage materials*

Spiropyrans are the most important photochromic and thermochromic molecules. They can be converted to a merocyanine dye by irradiation with UV light or heating (Fig. 5). The back

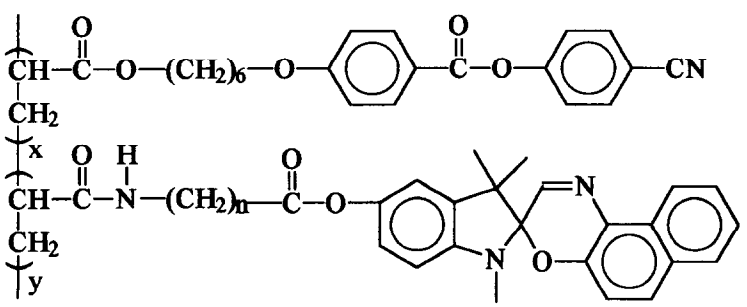


LCP-2

Fig. 6. The chemical structure of liquid-crystalline polyacrylates (LCP-2) containing spironaphthoxazine.

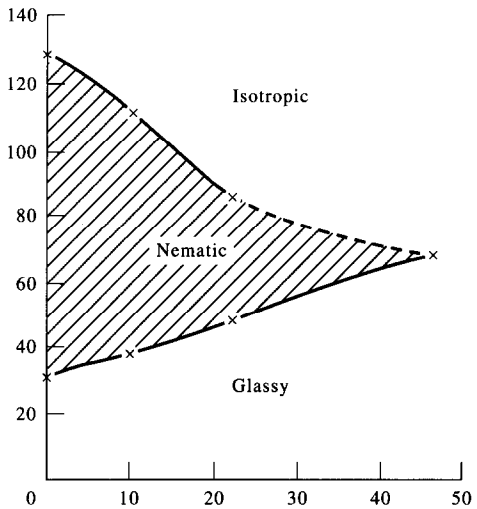


Fig. 7. Phase behavior of the spiropyran-containing polyacrylates (LCP-2) with $n = 5$. The composition of the polymers is given as mol% of spiropyran groups.[35]

reaction occurs spontaneously or on irradiation by visible light. Side-chain LC polyacrylates and polysiloxanes containing mesogenic and spiropyran side groups were first prepared by Cebrera and Krongauz in 1987.[31–33] Since then, studies on optical data storage on the basis of these kinds of photochromic polymer have attracted much attention in the past few years.[34–38]

An example of copolyacrylates containing 4-cyanophenyl benzoate and spiropyran side groups is given in Fig. 6. The obtained copolyacrylates reveal a nematic liquid-crystalline phase. The clearing temperatures decrease with increasing concentration of the spiropyran

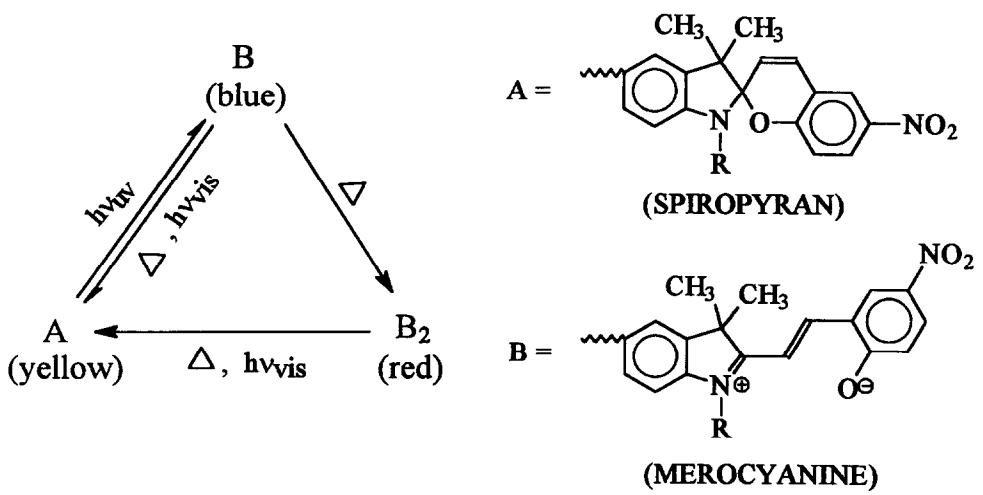


Fig. 8. Scheme for the conversion of the photochromic side groups.[35]

groups in the macromolecule. In some cases more than 30 mol% of spiropyran groups could be incorporated and mesomorphic behavior could still be observed (Fig. 7).

Irradiation of the polymer films with UV light at temperatures below the glass transition leads to formation of the blue color characteristic of the isolated merocyanine dye molecule. Above the glass transition temperature merocyanine dimers are formed, which are red. The spiropyran form of the photochrome with characteristic yellow color can be restored by irradiation of blue or red films with visible light. The color changes of the films are shown in Fig. 8. The thermal back reaction leading to equilibrium between spiropyran and merocyanine forms of the photochrome proceeds in the mesophase with a much lower rate than in the amorphous phase and is controlled by the viscosity of the polymer. In the liquid-crystalline glassy state the thermal reaction becomes extremely slow, or does not occur at all.

Natarajan *et al.*[39,40] recently reported the synthesis of a liquid-crystalline cyclic siloxane made up of photochromic spiropyran, biphenyl and cholesterol moieties. This siloxane formed a cholesteric film exhibiting selective reflection. These films were used to write,

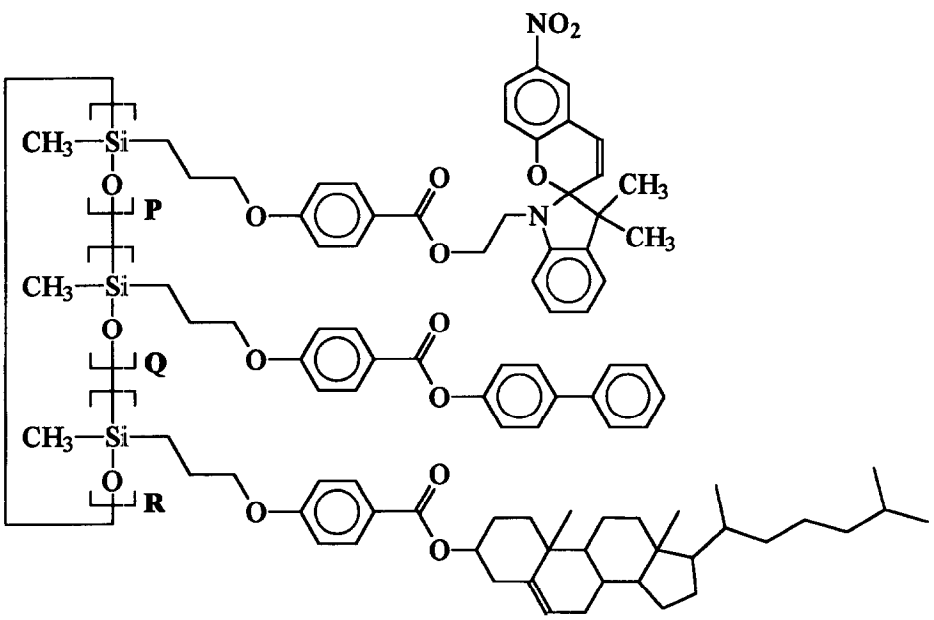


**P + Q + R = 5**

**A = P/5 : B = Q/5 : C = R/5**

| Compound | A/B/C ratio | Thermal transitions (°C) | Diffraction efficiency |
|---|---|---|---|
| 1 | 10/45/45 | g 62 n* 151 i | 0.15 |
| 2 | 20/40/40 | g 65 n* 170 i | 0.2 |
| 3 | 50/25/25 | g 80 viscous | 0.006 |

Fig. 9. Structure and thermal transitions of liquid-crystalline siloxane materials containing biphenylbenzoate, cholesteryl benzoate and spiropyranbenzoate side groups.[39]

erase and rewrite holograms.[39] Writing was achieved by UV laser light (358 nm), which led to opening of the closed spiropyran to the blue merocyanine form; heating to 60°C led to the disappearance of the blue color due to the formation of the closed form (Fig. 9).

### 2.3. *Conclusions*

Side-chain LCPs are undoubtedly promising materials for erasable optical data storage application. Nematic and smectic side-chain LCPs can be used for heat-mode recording owing to their various states of order and orientation capability. One simple method of presenting information optically is to generate an optical scattering center in an optically clear liquid-crystalline layer. However, heat-mode recording has the disadvantages of slow response time and low resolution. Side-chain LCPs containing azobenzene, spiropyran and fulgide moieties in the side groups can be used for photo-mode recording. The photochromic effect of dye moieties is responsible for reversible optical data storage. Their outlets in erasible holographic optical storage look particularly interesting. Nevertheless, at present, no side-chain LCP optical data storage product is available commercially. Evidently, more work needs be done before this can be realized. In the author's opinion, although further refinement in the synthesis of new materials with high purity and proper phase behavior is still required, more extensive studies on the processing and mechanical properties of these materials, coupled with a systematic investigation of the recording sensitivity, resolution and stability of the stored information for devices based on these materials, are even more important.

## 3. APPLICATION OF SIDE-CHAIN LCPS IN NON-LINEAR OPTICS

Non-linear optical (NLO) effects have attracted considerable attention from both fundamental and practical points of view. The major applications for non-linear optical effects include frequency conversion, light modulation, optical switching, optical logic, optical limiting and sensor protection.[41] All these applications require that the material have large optical non-linearities. Even though a number of inorganic crystals, such as KDP, KTP and $LiNbO_3$, are readily available for frequency-mixing applications, lack of good processability has kept them from being incorporated into integrated optical circuitry devices. In contrast, organic materials, in particular side-chain polymers, exhibit distinct advantages for applications in electro-optical devices because of their large optical non-linearity, relatively high damage threshold and good film-forming properties.

One of the simplest non-linear optical effects is second harmonic generation (SHG), i.e. doubling the frequency of laser beams as they pass through organic materials. In order to obtain a useful material for SHG, one requires the use of molecules with a large, microscopic, second-order non-linear hyperpolarizability tensor, $\beta$, organized in such a way that the resulting system has no center of symmetry, and an optimized constructive additivity of the molecular hyperpolarizability. It has been well established that molecules containing an electron donor and an electron acceptor attached to a $\pi$-conjugated system have a strong permanent dipole moment and present a large second-order non-linear hyperpolarizability. Since second-order (NLO) materials require a non-centrasymmetric structure, macroscopic organization of non-linear optical moieties in organic materials suitable for SHG applications

are currently obtained from single crystals, Langmuir–Blodgett multilayers and poled polymeric films. Growth of a single organic crystal is difficult in a thin film and Langmuir–Blodgett films induce important losses by scattering. Poled polymers seem to be the best candidates to meet the requirements for integrated non-linear optics, since they are compatible with semiconductor technology. Three classes of NLO polymers—i.e. amorphous polymers, side-chain liquid-crystalline polymers and ferroelectric side-chain polymers—have been investigated so far. In this section, the macroscopic second-order non-linear suceptibility, $\chi^{(2)}$, values of side-chain LC polymers and ferroelectric side-chain LC polymers are discussed.

### 3.1. *Side-chain LC polymers*

In 1982, Meredith *et al.*[42] demonstrated that a large second-order NLO coefficient can be obtained for a poled film consisting of a nematic side-chain LC polymethacrylate doped (2% by weight) with the NLO dye 4-(dimethylamino)-4′-nitrostilbene (DANS). The SHG was considerably larger (100 times) than that which could be obtained with a 2% DANS-doped poly(methyl methacrylate) sample. However, two disadvantages are considered for dye-doped side-chain LCP systems. One is the limit solubility of the dye molecules in the LCP matrix; concentrations of up to a few percent only are possible. The other is the difficulty in keeping the orientation owing to the fairly low $T_g$ ( $< 50°C$) of the LCP host.

For these reasons of stability and concentration of the dopant, many researchers have synthesized side-chain LC copolymers bearing the NLO-active dye as side groups.[43–58] We describe some of these results reported after 1989.

McCulloch and Bailey have reported the copolymers shown in Fig. 10[44] and have measured $d_{33}$ of the order of 8 pm $V^{-1}$ at 1.319 $\mu$m with corona poling. Amano and co-workers[45,46] have found that $\chi^{(2)}$ values of side-chain LCPs are higher than for the corresponding amorphous polymers (see Fig. 11). Smith and Coles[52] have reported the second- and third-order non-linear optical susceptibilities of 10 donor–acceptor substituted side-chain LCPs (see Table 1). Recently, Hsieh *et al.* succeeded in synthesizing some side-chain LCPs with tolane-based NLO-active groups (see Fig. 12) and have obtained better results.[57,58] The measured $d_{33}$ was of the order of 22 pm $V^{-1}$ at 1.06 $\mu$m with corona poling.

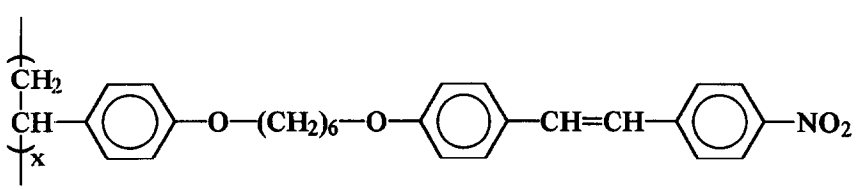


**g 85 $S_A$ 165 I**

**$T_P$ = 50 C (Corona)**
**$d_{33}$ = 8.4 pmV$^{-1}$**
**$\lambda$ = 1.319 $\mu$m**

Fig. 10. A side-chain LC polystyrene synthesized for $\chi^{(2)}$ measurement. Poling is made by corona at a temperature $T_p = 50°C$.[44]

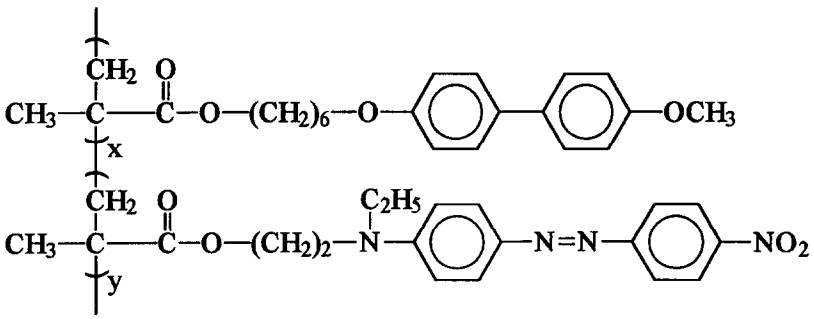


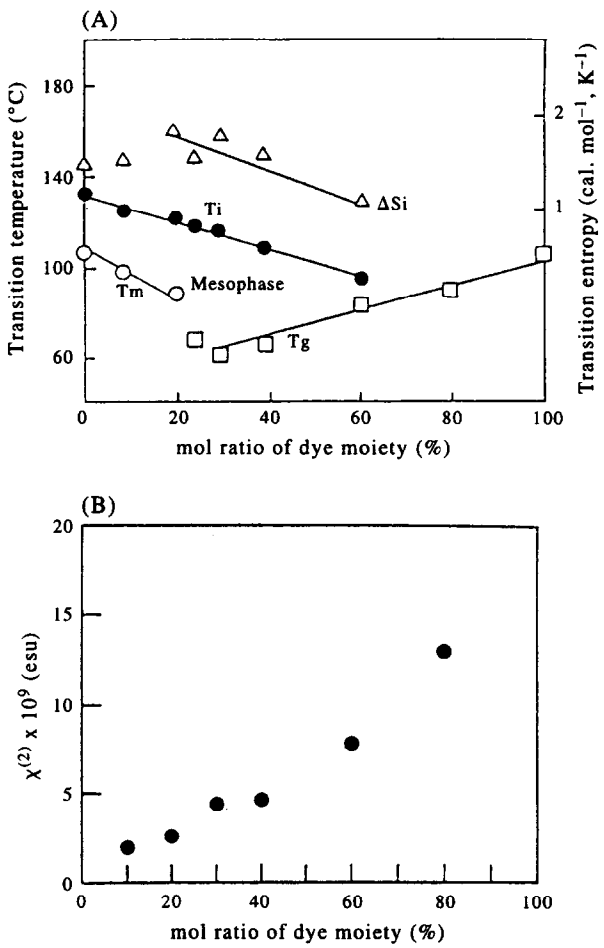


Fig. 11. Thermal transitions (A) and variation of $\chi^{(2)}$ values (B) versus the mole ratio of dye moiety in the side-chain LC copolymethacrylates.[46]

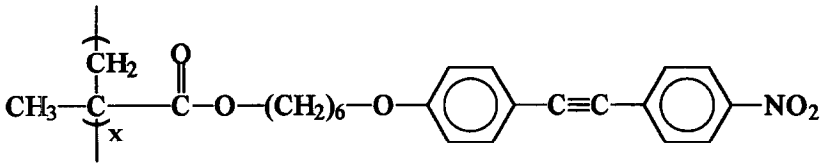


g 47.7 n 78.6 I
$\lambda_{max}$ = 357 nm, $T_P$ = 60°C (Corona)
$d_{33}$ = 22.6 pmV$^{-1}$

Fig. 12. A side-chain LC polymethacrylate synthesized for $\chi^{(2)}$ measurement. Poling is made by corona at a temperature $T_p$ = 60°C.[58]

### 3.2. *Ferroelectric side-chain LC polymers*

It is well known the chiral smectic C ($S_C$*) phase possesses a ferroelectric smectic layer[59] but, owing to the helicoidal superstructure of the $S_C$* phase, no macroscopic ferroelectricity only helioelectricity occurs. Only an unwinding of this helicoidal structure yields a sample with a macrosopic spontaneous polarization exhibiting $C_2$ point symmetry. The $C_2$ symmetry implies that the untwisted $S_C$* phase can exhibit second-order non-linear properties. However, the second-order NLO response of ferroelectric liquid crystals (FLCs) turned out to be rather small compared with that of standard NLO-active materials.[60] This is only because of the molecular structure of the mesogens commonly used. They have no donor and acceptor groups oriented along the direction of the polar axis. More recently, higher non-linear susceptibility on special molecular-designed FLCs were reported.[61–63]

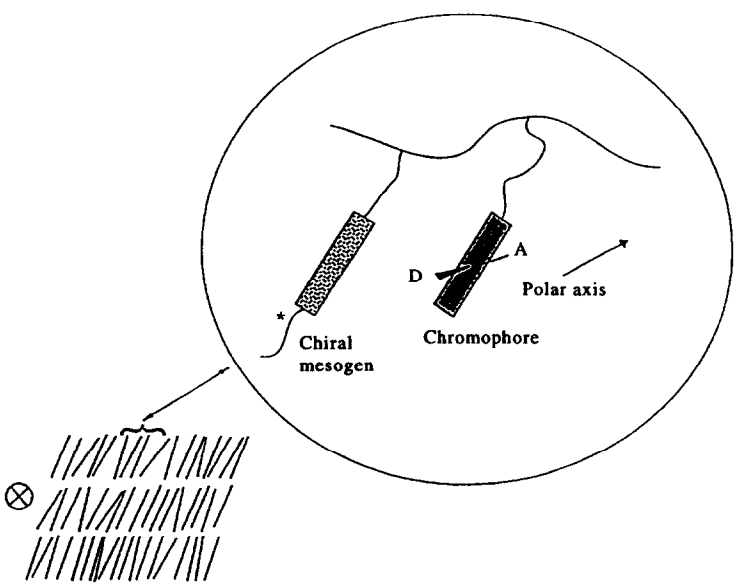


Fig. 13. Schematic representation of chiral smectic C* layers in the helix-unwound state. The inset shows the orientation of the achiral chromophores in the ferroelectric matrix.

Table 1. The material phases, structures and second- and third-order non-linear optical susceptibilities measured at 1064 nm and 1579 nm

| Material and phase behavior | Structure | 1064 nm | | | 1579 nm |
|---|---|---|---|---|---|
| | | $\chi^{(2)}_{33} \times 10^{9}$ (esu) | $\chi^{(2)}_{31} \times 10^{-9}$ (esu) | $\chi^{(3)} \times 10^{-13}$ (esu) | $\chi^{(3)} \times 10^{-13}$ (esu) |
| A<br>G 50°C M 160°C I<br>$x = 11$ | 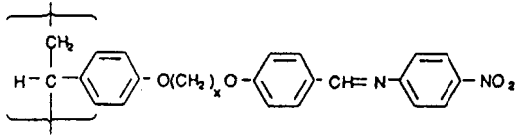 | 6.30 ± 1.58 | 1.90 ± 0.48 | 22.0 ± 3.3 | 13.1 ± 2.0 |
| B<br>G 120°C N 150°C I | 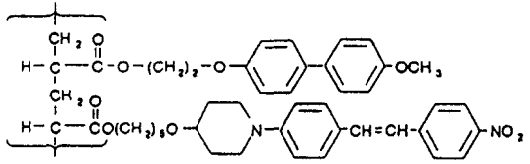 | 6.00 ± 1.50 | 1.24 ± 0.31 | — | — |
| C<br>G 32°C M 80°C $S_A$<br>124.5°C N 132°C I | 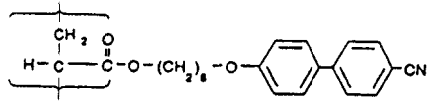 | 3.36 ± 0.84 | 0.62 ± 0.16 | 3.7 ± 0.6 | 1.2 ± 0.2 |
| D<br>G 40.5°C N 104°C I | 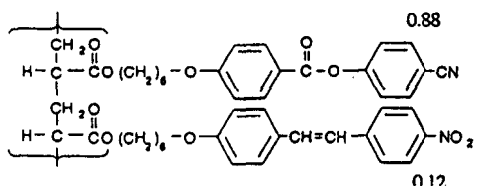 | 3.00 ± 0.75 | 0.87 ± 0.22 | — | — |
| E<br>G 110°C I | 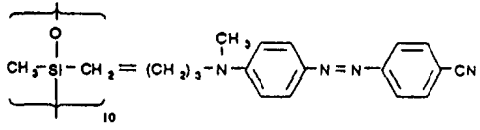 | 2.55 ± 0.64 | 0.86 ± 0.22 | 58.0 ± 8.7 | 5.6 ± 0.8 |

| | | | | | |
|---|---|---|---|---|---|
| F<br>G 30°C S 125°C I | 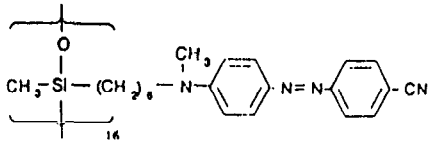 | 1.89 ± 0.47 | 0.47 ± 0.12 | 53.4 ± 8.0 | 10.01 ± 1.5 |
| G<br>G 84°C N 113.5°C I | 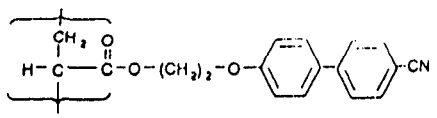 | 1.30 ± 0.33 | 0.23 ± 0.06 | — | — |
| H<br>G 30°C $S_A$ 145°C I | 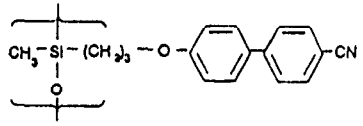 | 0.55 ± 0.14 | 0.13 ± 0.03 | 4.6 ± 0.7 | 0.6 ± 0.1 |
| I<br>C 59°C $S_A$ 110°C I | 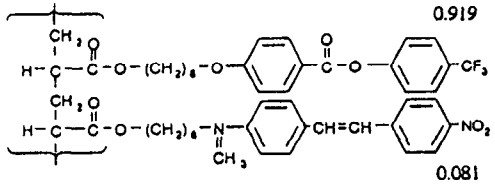 | 0.25 ± 0.06 | 0.06 ± 0.01 | 4.0 ± 0.6 | 1.3 ± 0.2 |
| J<br>C 14°C$S_A$ 90°C N<br>107.5°C I | 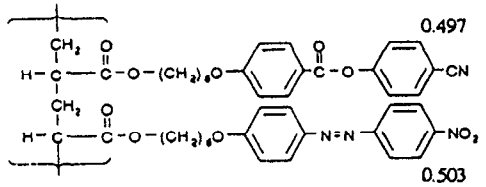 | — | — | 16.1 ± 2.4 | 3.2 ± 0.5 |

Table 1. Continued.

| Material and phase behavior | Structure | 1064 nm | | | 1579 nm |
|---|---|---|---|---|---|
| | | $\chi^{(2)}_{33} \times 10^{9}$ (esu) | $\chi^{(2)}_{31} \times 10^{-9}$ (esu) | $\chi^{(3)} \times 10^{-13}$ (esu) | $\chi^{(3)} \times 10^{-13}$ (esu) |
| K<br>G 10°C M 90°C I | 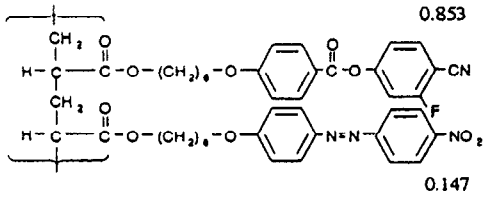 | — | — | 3.5 ± 0.5 | 2.1 ± 0.3 |
| L<br>G ? $S_A$ 65°C N 100°C I | 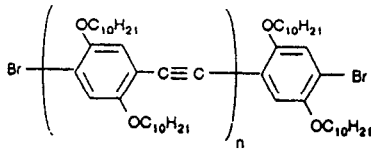 <br>where $3 \leqslant n \geqslant 150$ | — | — | 35 ± 5.0 | 21 ± 3.0 |

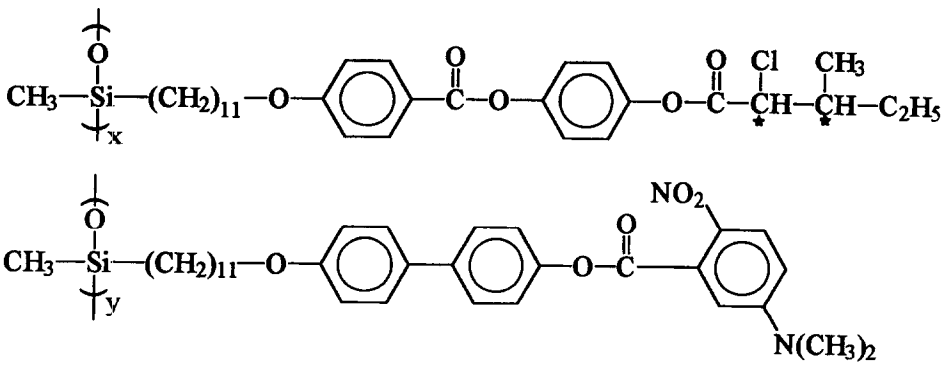

x : y = 80 : 20

g -14 $S_C$* 68 $S_A$ 83 i

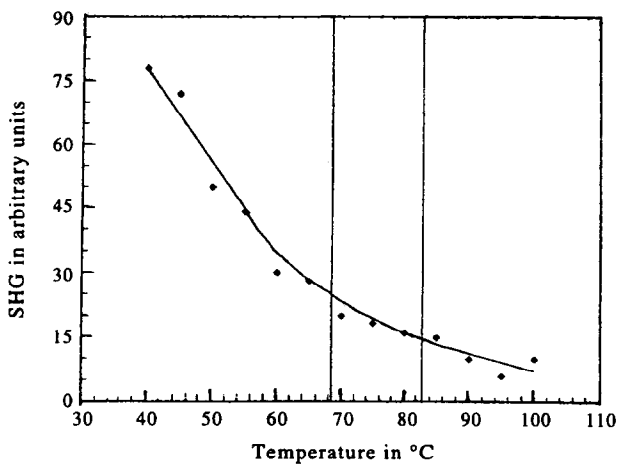


Fig. 14. Dependence of the second-order signal on temperature for a ferroelectric side-chain LC copolysiloxane.[68]

The NLO effects of some ferroelectric side-chain LC polymers have also been demonstrated recently.[64–70] Zental and co-workers[67] have reported on ferroelectric side-chain LC copolymers containing NLO-active chromophores (see Figs 13 and 14) which show considerably higher SHG activity than the homopolymer without chromophores. Finkelmann's group has even demonstrated the mechanical-induced SHG in $S_C$* elastomers.[69,70]

### 3.3. *Conclusions*

Side-chain LCPs have been proved to be a promising class of polymeric materials for nonlinear optical applications. Most of the side-chain LC copolymers containing NLO chromophores in the side groups show much higher SHG values than that of KDP. However, a

critical stage in the processing of these polymers for use in non-linear optics is the director alignment of NLO chromophores in an electric field. Unfortunately, NLO chromphores having a strong permanent dipole moment tend to form anti-parallel correlations in the liquid-crystalline states. Therefore, the second-order NLO potential of side-chain LCPs is restricted by the poor degree of poled order which can be obtained. Some studies indicate that a significant increase in the subsceptibility values can be expected if a large poling field can be applied without damaging the material. In the author's opinion, poling of these materials by a magnetic field could be a good selection in order to avoid this damage.[71] Furthermore, the side-chain LCPs possess a major disadvantage over inorganic crystals with respect to long-term NLO thermal stability. When the poling electric field is removed, the dipole orientation in the poled polymers tends to relax back to the thermodynamically more stable random structure through polymer-chain segmental motions and pendant rotations, leading to the decay of second-order NLO activity. Because of this, the electro-optic applications of poled polymers are greatly limited since practical devices applications require long-term stability of NLO activity at normal circuit working temperature, which ranges from 90°C to 125°C. For a side-chain LCP, it usually needs a flexible spacer in order to form a mesophese. Owing to the plasticizer effect, the flexible spacer will decrease the $T_g$ of a side-chain LCP. Therefore most of the side-chain LCPs synthesized for NLO measurements show relatively low $T_g$ ( $< 50$°C). In developing high $T_g$ side-chain LCPs, two approaches can be considered. One approach is to use a more rigid polymer backbone for the side-chain LCP. The other approach, in the author's opinion, is to use a double-end crosslinkable LC system[72] in order to from a crosslinked LC network with NLO-active groups.

## 4. SIDE-CHAIN LCPS USED AS STATIONARY PHASES FOR GAS CHROMATOGRAPHY, SUPERCRITICAL-FLUID CHROMATOGRAPHY AND HIGH-PERFORMANCE LIQUID CHROMATOGRAPHY

### 4.1. *Introduction*

The use of liquid crystals as the stationary phase in gas chromatography (GC) was first reported by Kelker in 1963. This field has been extensively reviewed.[73,74] Unlike conventional stationary phases that provide separation based on solute vapor pressure and/or different solubility arising from specific energetic interactions, liquid crystal stationary phases yield separation based upon differences in solute molecular shape. Although the properties exhibited by many monomeric liquid crystals are good from the point of view of GC requirements, polymeric liquid crystals are attracting growing attention because they offer significant improvements in column efficiency, as well as thermal stability, over low-molar-mass liquid crystals. Among liquid crystal polymers, polysiloxanes are particularly useful as stationary phases. Finkelmann *et al.* first used this type kind of polymer as GC stationary phases.[75] These polymers are referred to as mesomorphic polysiloxanes (MEPSIL). The applications of MEPSIL solvents as GC stationary phases have been extensively reviewed by Janini *et al.*[76] and by Witkiewicz.[77,78] A few examples of side-chain LC polyacrylates[79–81] have also been reported as stationary phases for GC. After 1988, the quantity of publications concerning the applications of side-chain LCPs as GC stationary phase decreased remarkably. On the other hand, more studies are aimed to the applications of side-chain LCPs in

supercritical-fluid chromatography (SFC)[82–84] and high-performance liquid chromatography (HPLC).[85–92] Here, we do not intend to review all of them. The following sections will emphasize some representative examples of the recent progress in these fields.

### 4.2. *Side-chain LCPs with a broad temperature ranges of cholesteric phase or chiral smectic C phase used as GC stationary phases*

Many of the side-chain LCPs stationary phases tend to form nematic and smectic phases over a broad temperature ranges. Only a very few cholesteric or ferroelectric polymeric liquid crystals have been found that exhibit good properties as GC stationary phases. LC copolysiloxanes containing cholesterol moieties in the side groups were prepared by Master *et al.*[93] Depending on the concentration of cholesteric moieties, the copolymers are able to form nematic, cholesteric and smectic phase, respectively (see Fig. 15). The copolymer with broad temperature range of cholesteric phase was found to offer better performance as stationary phase than those with nematic and smectic phases (Fig. 16).

A ferroelectric and a cholesteric side-chain LC polysiloxane which were used as GC stationary phase over a wide temperature range were reported by Lin and Hsu.[94] The chemical structures and mesomorphic properties of both polysiloxanes, LCP-3 and LCP-4, are presented in Fig. 17. The capillary columns that were coated with polymers LCP-3 and LCP-4

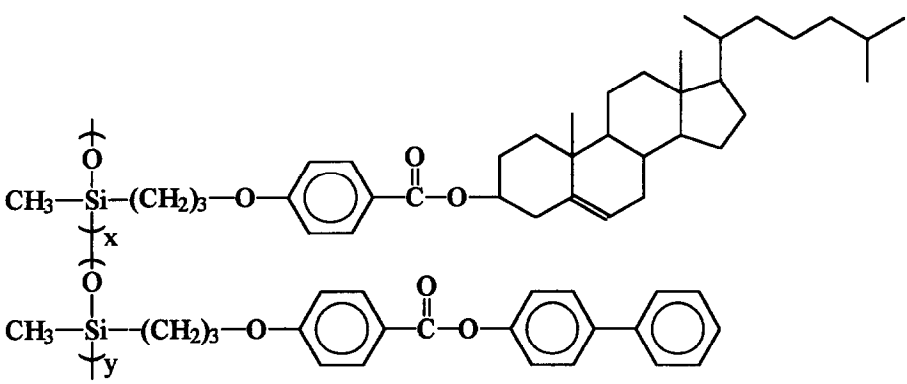


Thermal transitions of LC copolysiloxanes

| Copolymer | *x*/*y* | Thermal transition (°C) |
|---|---|---|
| A | 0/100 | K 55 n 175 i |
| B | 25/75 | g 50 n* 210 i |
| C | 50/50 | g 62 n* 230 i |
| D | 75/25 | g 50 S > 230 dec |
| E | 100/0 | g 72 S > 250 dec |

Fig. 15. Chemical structure and phase transitions of side-chain LC copoysiloxanes A–E.

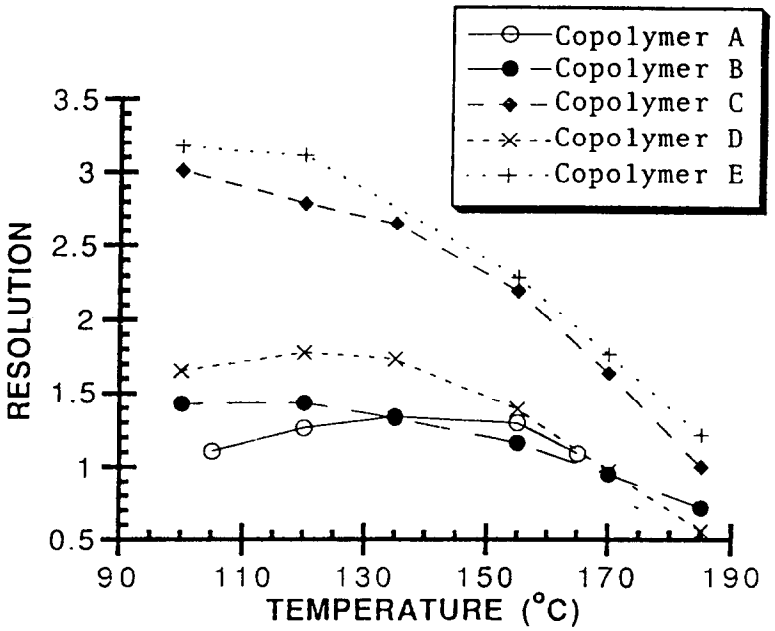


Fig. 16. Resolution versus temperature (°C) for anthracene and phenanthracene columns coated with stationary phases A–E.

are termed LC-1 and LC-2, respectively. Column LC-1 containing LCP-3 yields about 2100 plates/m, while LC-2 column containing LCP-4 yields about 2340 plates/m (triphenylene, 230 °C). Both columns were found to provide satisfactory column efficiency (see chromatograms presented below).

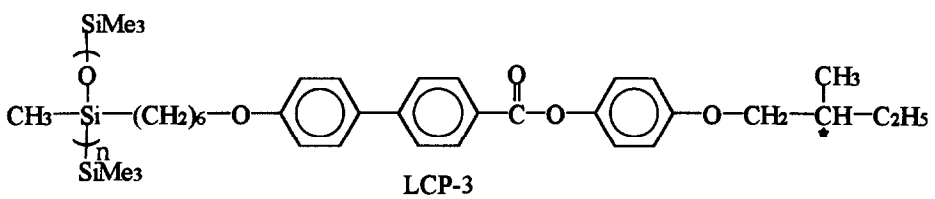


LCP-3

G 16 $S_B$ 120 $S_C^*$ 166 $S_A$ 244 I

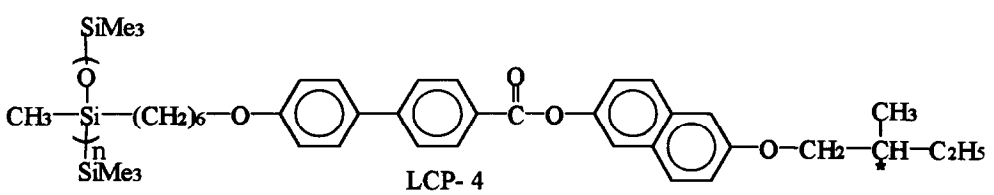


LCP- 4

G 12 $N^*$ 319 I

Fig. 17. Chemical structures and phase transitions of side-chain LC polysiloxanes LCP-3 and LCP-4.

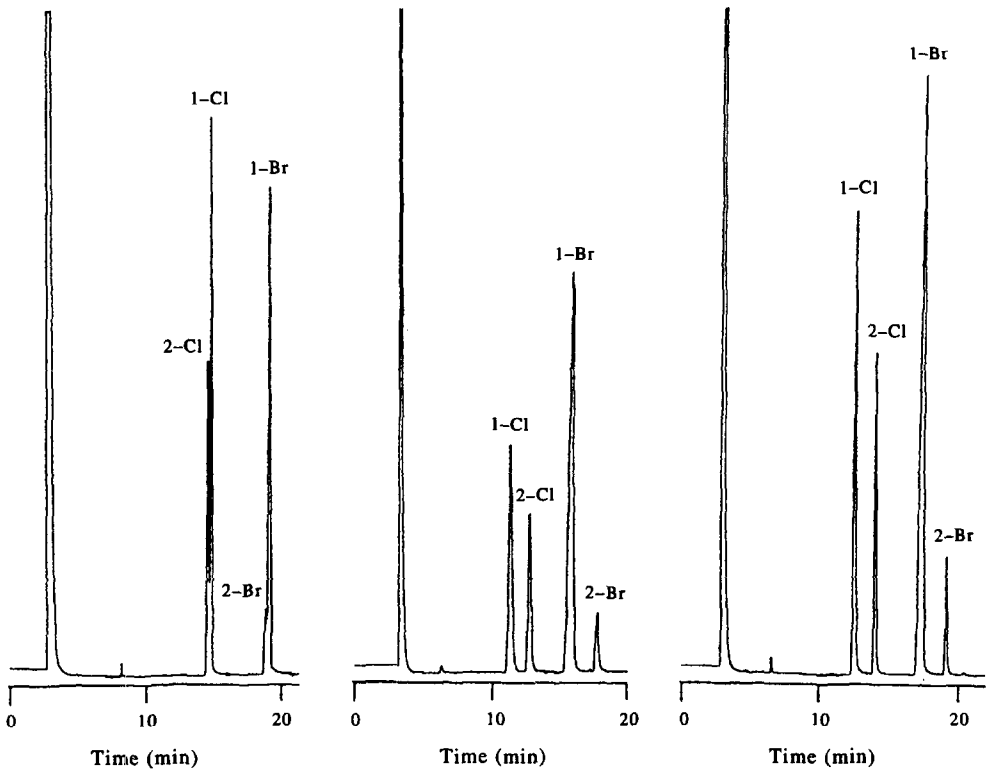


Fig. 18. Chromatograms of 1- and 2-chloronaphthalenes on (A) SE-54, (B) LC-1 and (C) LC-2. Temperature was programmed from 130°C to 200°C at 2°C/min.

The separations of two pairs of halogenated naphthalene isomers on SE-54, LC-1 and LC-2 columns are illustrated in Fig. 18. Both LC-1 and LC-2 columns show much better selectivity for the two pairs of halogenated naphthalene isomers than the SE-54 column.

The separations of some fatty acid methyl esters on LC-1 and LC-2 columns are presented in Fig. 19(B) and Fig. 19(C). The order of elution is remarkable when compared with that generally observed with the OV-210 column [see Fig. 19(A)]. First, the *cis* and *trans* isomers are better resolved on both LC-1 and LC-2 columns. Second, the *trans* isomers are retained longer than the corresponding *cis* isomers of the same carbon number, which is the reverse of that observed with the OV-210 column. Furthermore, the compounds are eluted in order of increasing carbon number and, for each group of compounds having the same carbon number, the elution time increases with increasing saturation.

The programed-temperature separation of two-, three-, four- and five-ringed polycyclic aromatic hydrocarbons (PAHs) with column LC-2 is presented in Fig. 20. More than 31 kinds of PAH compound, which are summarized in Table 2, have been eluted. The elution pattern of these solutes with mesomorphic polysiloxane is consistent with the degree of their rod-like geometry, the more rod-like being retained for longer. For example, phenanthrene ($L/B$ = 1.46) elutes earlier than anthrancene ($L/B$ = 1.56), benza[*a*]anthracene ($L/B$ = 1.58) elutes

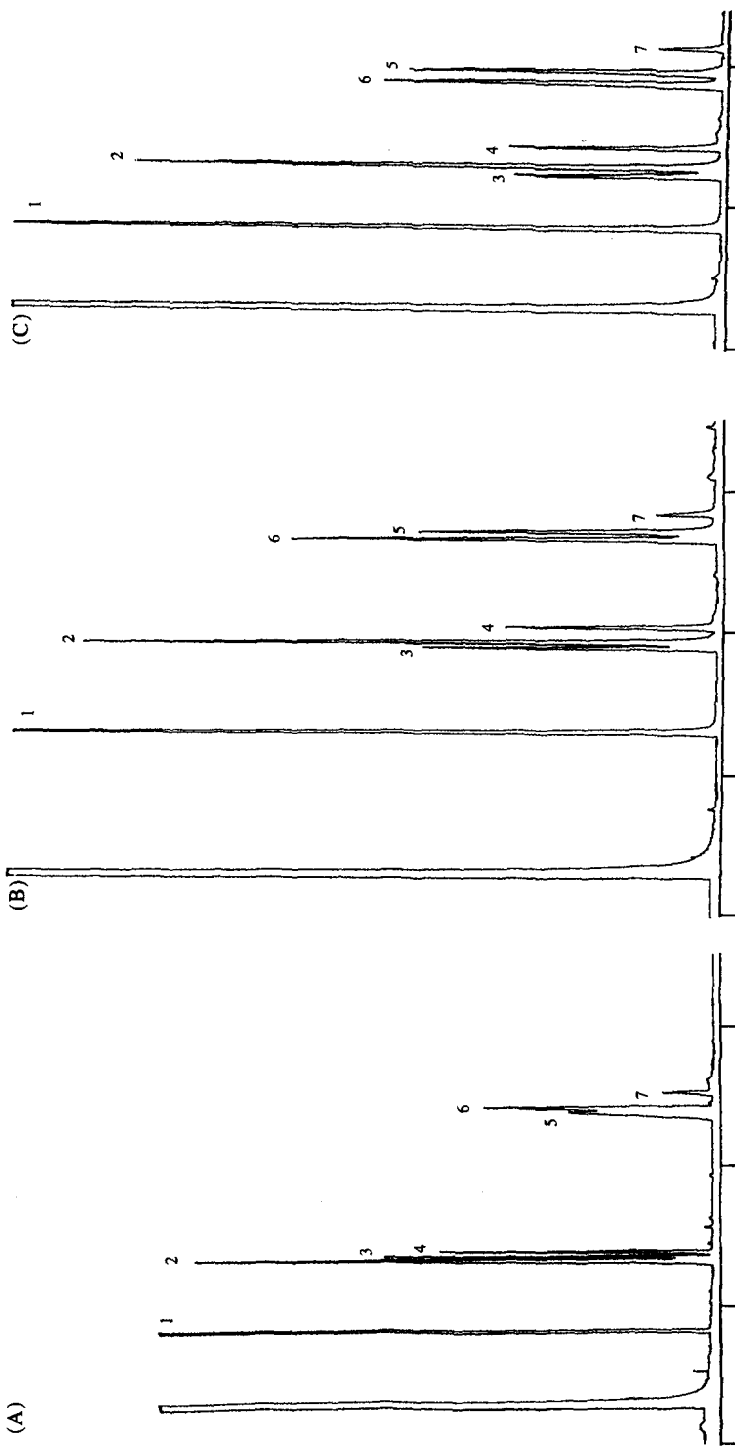


Fig. 19. Chromatograms of fatty methyl esters on (A) OV-210 (column temperature, 160°C; isothermal), (B) LC-1 and (C) LC-2. Temperature was programmed from 130°C to 200°C at 2°C/min for (B) and (C). Peaks: 1, myristic; 2, palmitelaidic; 3, palmitoleic; 4, palmitoleic; 5, elaidic; 6, oleic; 7, steric.

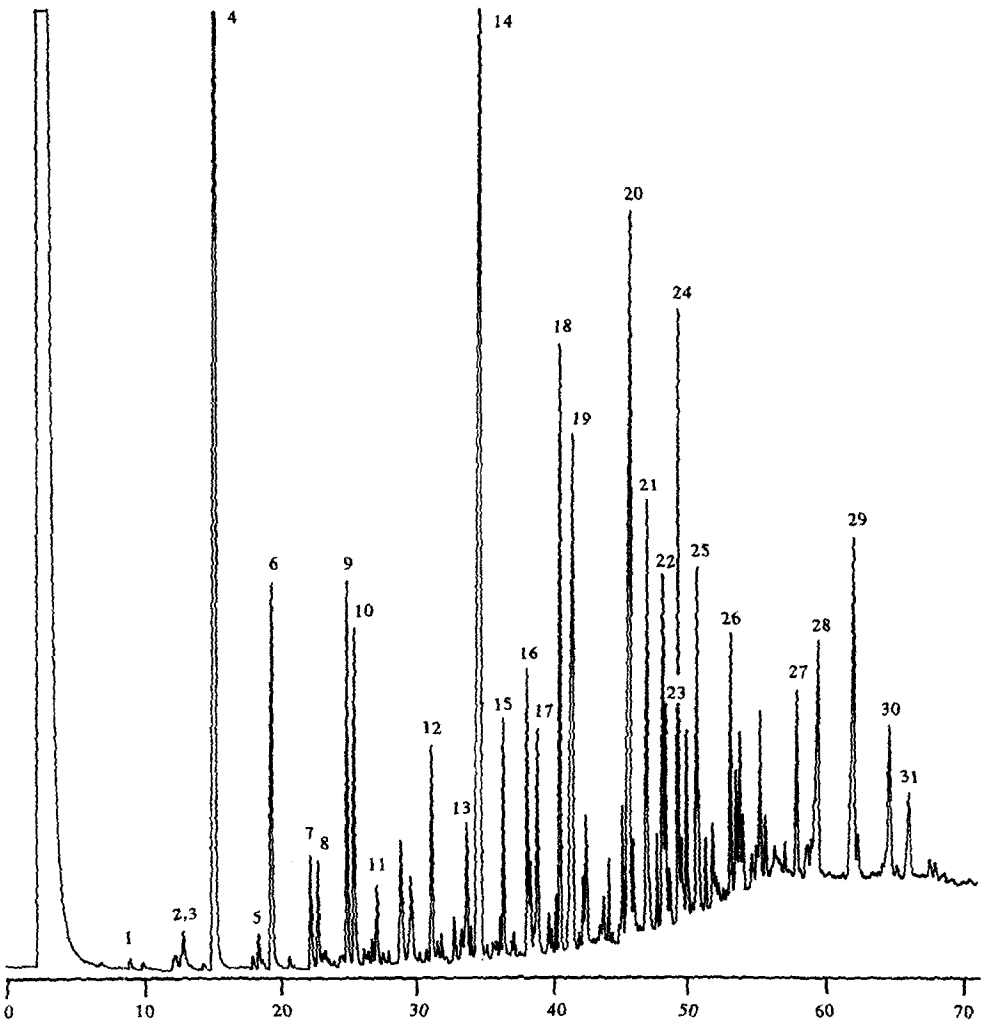


Fig. 20. Chromatograms of 31 kinds of PAH compound on LC-2. Temperature was programmed from 110°C to 280°C at 3.5°C/min.

earlier than chrysene ($L/B = 1.72$). Among *o*-, *m*- and *p*-terphenyls, *o*-terphenyl ($L/B = 1.10$) elutes first, followed by *m*-terphenyl ($L/B = 1.47$) and then *p*-terphenyl ($L/B = 2.34$).

In conclusion, the side-chain liquid-crystalline polysiloxanes with wide temperature range of chiral smectic or cholesteric phases have been proved to be useful in separating many classes of compound. The polymers obtained show very high thermal stability. Because the separation is based on molecular shape, isomers that have very similar intrinsic properties can be separated by these kinds of mesomorphic polymer stationary phase. Both prepared columns show very high column efficiency for all four separation systems. The results may be attributed to the twisted packing structure of chiral smectic or cholesteric mesophase exhibited by the stationary phases.

Table 2. Peak assignments for PAH compounds and their identification methods

| Peak no. | Compound | Molecular weight | Identification method* |
|---|---|---|---|
| 1 | Naphthalene | 128 | a, b |
| 2 | 2-Methylnaphthalene | 142 | a, b |
| 3 | 1-Methylnaphthalene | 142 | a, b |
| 4 | Biphenyl | 154 | a, b |
| 5 | Biphenylene | 152 | a, c |
| 6 | Acenaphthylene | 152 | a, b |
| 7 | Dibenzofuran | 168 | a |
| 8 | 9-Methylene-9H-fluorene or 1,1′-(1,2-ethynediyl)-bis benzene or 2,3-diphenyl-2-cyclopropen-l-one | 178 | a |
| 9 | Same as 8 | 178 | a |
| 10 | Fluorene | 166 | a, b |
| 11 | *o*-Terphenyl | 230 | a, c |
| 12 | 1-Phenylnaphthalene | 204 | a, b |
| 13 | Same as 8 | 178 | a |
| 14 | Phenanthrene | 178 | a, b |
| 15 | Anthracene | 178 | a, b |
| 16 | 4H-Cyclopenta[*def*] phenanthrene | 190 | a |
| 17 | 1-Methylanthracene | 192 | a |
| 18 | 2-Phenylnaphthalene | 204 | a, b |
| 19 | *m*-Terphenyl | 230 | a, c |
| 20 | Fluoranthene | 202 | a, b |
| 21 | Acephenanthrylene | 202 | a, b |
| 22 | Pyrene | 202 | a, b |
| 23 | Benzo[*c*]phenanthrene | 228 | a |
| 24 | *p*-Terphenyl | 230 | a, c |
| 25 | 11H-Benzo[*a*]fluorene or 11H-benzo[*b*]fluorene | 216 | a |
| 26 | 1,2′-Binaphthalene or 1,1′-binaphthalene or 9-(phenylmethylene)-9H-fluorene | 254 | a |
| 27 | Benzo[*ghi*]fluoranthene | 226 | a, c |
| 28 | Triphenylene or naphthacene | 228 | a |
| 29 | Benzo[*a*]anthracene | 228 | a, b |
| 30 | Chrysene 448° | 228 | a, b |
| 31 | 1,2′-Binaphthalene or 1,1′-binaphthalene or 2,2′-binaphthalene | 254 | a |

*Identification method: a, by sample mass spectra; b, by retention index and standard injected into GC; c, by retention index published in [57–59].

### 4.3. *Side-chain LC polysiloxanes containing crown ether moieties used as GC stationary phases*

Side-chain LCPs containing crown ether moieties in the side groups have been prepared by Percec and Rodenhouse[95] and Hsu *et al.*[96,97] The application of crown-ether-containing side-chain LC polysiloxanes in GC stationary phases was presented by Fu *et al.*[98,99] An example of separations of methylnaphthalenes and dinitrotoluene with this kind of LCP stationary phase is shown in Fig. 21. The results demonstrate the superior selectivity of the crown ether for the separation of structural isomers of methylnaphthalene and dinitrotoluene.

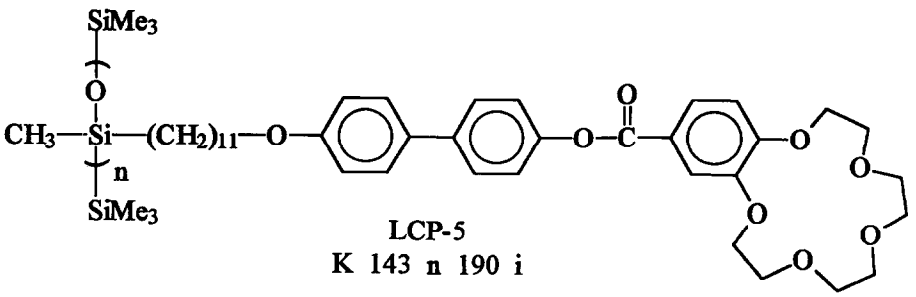


LCP-5
K 143 n 190 i

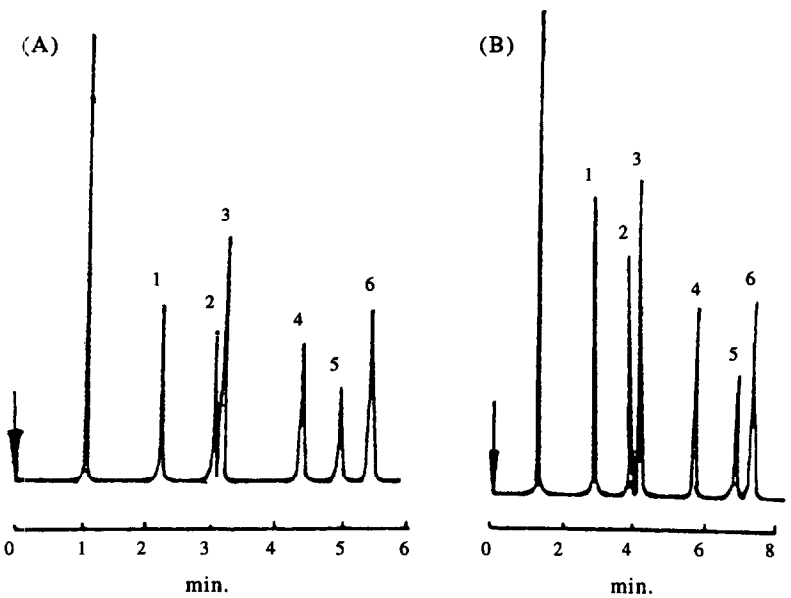


Fig. 21. (A) Chromatograms of substituted naphthalenes on LCP-5 columns at 160°C. Peaks: 1, naphthalene; 2, 2-methylnaphthalene; 3, 1-methylnaphthalene; 4, 2,6-dimethylnaphthalene; 5, 1,5-dimethylnaphthalene. (B) Chromatograms of dinitrotoluene (DNT) isomers on LCP-5 columns at 180°C. Peaks: 1, 2,6-DNT; 2, 2,5-DNT; 3, 2,3-DNT; 4, 2,4-DNT; 5, 3,5-DNT; 6, 3,4-DNT.

### 4.4. *Application of side-chain LCPs as SFC stationary phases*

Side-chain LCP stationary phases in capillary columns have also been applied in supercritical-fluid chromatography.[82–84] In the previous section, unsurpassed resolution of isomeric PAHs has been demonstrated with GC by using side-chain LCPs as the stationary phase. However, the thermal instability of these phases precludes continuous operation at temperatures much higher than 280°C and therefore limits their use for analysis of high-molecular-weight PAHs. SFC has became a popular analytical tool not only for its ability to analyse thermal unstable and relatively high-molecular-weight compounds, but also because highly efficient and selective capillary columns can be used to achieve unique separation.

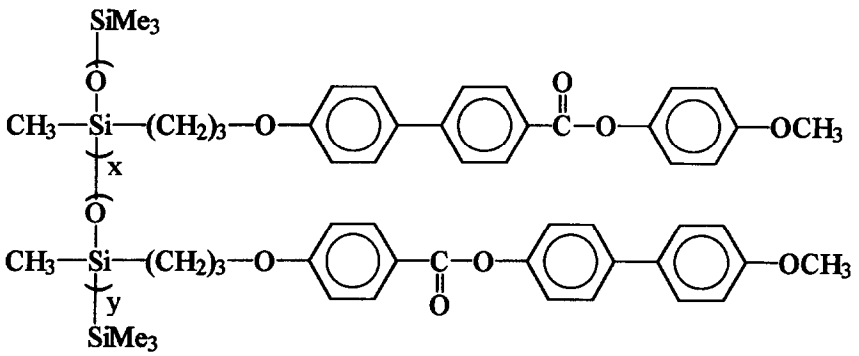


Fig. 22. Chemical structure and phase transition of a side-chain LC polysiloxane.

Because the separation can be achieved at lower temperatures in SFC compared with GC, the resulting selectivity is usually higher. In 1988, Lee *et al.* used an LC polysiloxane (see Fig. 22) as an SFC stationary phase to separate petroleum hydrocarbons. It is found that the resolution of PAHs is greater in SFC than in GC with the same LCP stationary phase (see Fig. 23).

### 4.5. *Application of side-chain LCPs as HPLC stationary phases*

In contrast to the many publications concerning side-chain LCPs for GC, there have been few reports of their use as stationary phases in HPLC.[85,86] In HPLC, however, it was necessary for the liquid crystals to be chemically bonded to the solid support via a chemical reaction in order to achieve the stability required for a long column lifetime, which was adversely affected by solubility under the normal mobile phase solvent conditions.[87–92]

The concept of bonding a liquid crystal material to a solid support like silica via well-established organosilane chemistry has proved to be a viable method.[87] An example of a successful bonding scheme is shown in Fig. 24. This method utilizes a standard approach in organosilane chemistry, involving the synthesis of a silanization reagent by reaction of dimethylchlorosilane with a terminal olefin compound.

The liquid crystal bonded phases have been evaluated by using cyclic aromatic hydrocarbon (PAHs) as the probe samples in reversed-phase HPLC.[92] The results clearly indicate that these phases have better planarity and shape recognition than commercially available polymeric octadecylsilica (ODS) phases whose strong planarity and shape selectivity were found earlier.

The first example of side-chain LCPs used as stationary phase for HPLC was demonstrated by Klein and Springer in 1991.[85,86] A series of side-chain LC polyacrylates, containing 4-methoxyphenyl benzoate moieties as mesogenic units and aliphatic spacers containing two to six methylene units, were coated onto silica gels. These side-chain LCP modified silica gels served as stationary phases in HPLC. Steroid and dinitrobenzene isomers were used as

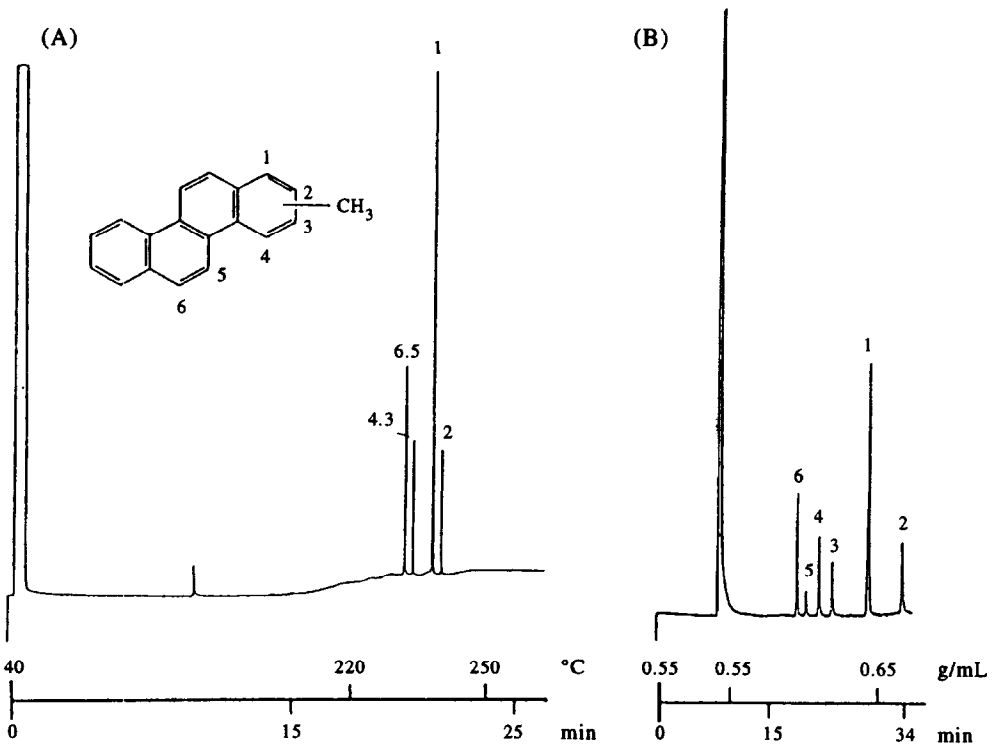


Fig. 23. Chromatograms of six methylchrysenes on the same liquid-crystalline stationary phase in (A) GC (200 $\mu$m i.d. column) and (B) SFC (50 $\mu$m i.d. column). GC conditions: temperature programmed from 40°C to 200°C at 10°C/min, then at 4°C/min to 240°C. SFC conditions: density programmed from 0.55 g/ml to 0.70 g/ml at 0.005 g/ml min after a 10 min isoconfertic period; temperature held at 100°C. Peak numbers represent the position of methyl substitution on the chrysene structure.

sample substances for testing the chromatographic properties of these stationary phases. The results demonstrated that, in analogy to gas chromatography, separations based on the mesophase structure can be observed also in high-performance liquid chromatography.

### 4.6. *Conclusion*

Side-chain LCP stationary phases have been found to be useful in separating many classes of compounds. Because the basis of separation is molecular shape, isomers that have very similar intrinsic properties can be separated with this kind of stationary phase. The high selectivity makes the use of side-chain LCP stationary phases a suitable option for GC, SFC and HPLC. To date, many side-chain LCPs with wide temperature ranges of nematic and smectic phases have been proved to be useful as stationary phases. Side-chain LCPs with chlolesteric and chiral smectic C phases are also known, although to a much smaller extent. New side-chain LCPs are continuously becoming available and it is believed that the best of them are not yet to come. For instance, side-chain LCP with discotic phases have not so far

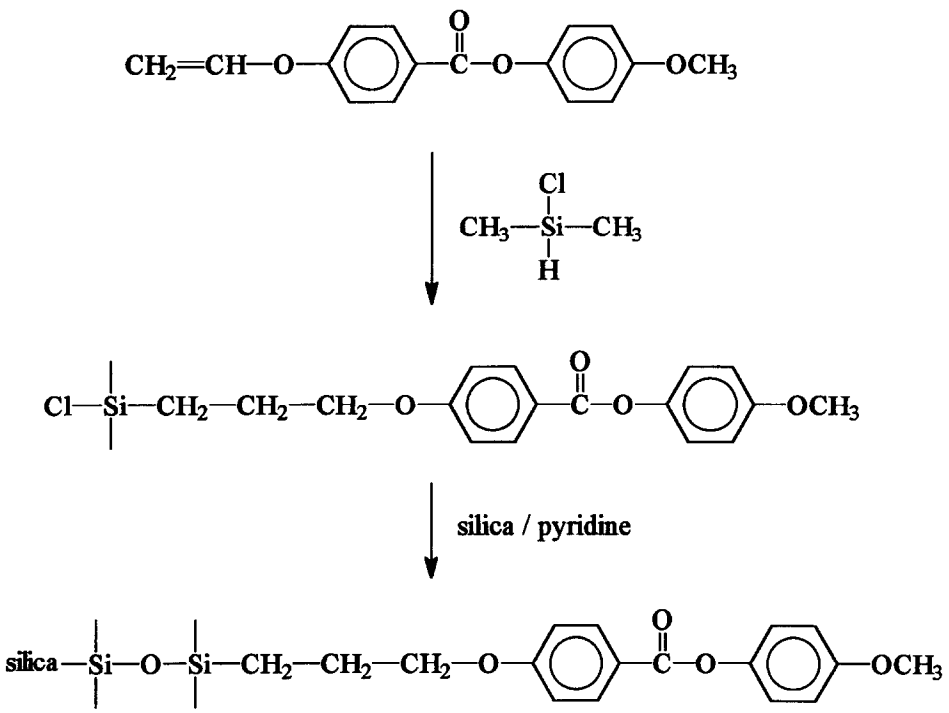


Fig. 24. Reaction scheme for the bonding of [4-(allyloxy)benzoyl-4-methoxyphenyl] to silica.

been tested as stationary phases. Since low-molar-mass discotic liquid crystals are useful, the discotic side-chain LCPs have the potential to become excellent stationary phases.

## 5. THE APPLICATION OF SIDE-CHAIN LCPS AS SEPARATION MEMBRANES

Non-porous polymeric membranes are important for the separation of mixtures. For the practical application of non-porous membranes, it is desirable to have a high selectivity combined with a maximum permeability. Semicrystalline or glassy polymeric membranes often show good selectivity owing to their ordered or stiff structures, but low permeability. On the other hand, membranes in the liquid state exhibit high permeability but poor selectivity. The liquid-crystalline polymers are expected to have high chain mobility in the LC states. This provides an enhanced transport velocity of gas molecules through LC membranes. However, in the LC states the anisotropic LC structures reduce the amplitude of polymer-chain mobility compared with the isotropic state, which should lead to an enhanced selectivity between small and bulky gas molecules.

To date, investigations of transport properties of membranes in the LC state have been made by seveal research groups.[98–116] Kajiyama and co-workers[98–101] have studied gas transport properties through low-molar-mass liquid crystal/polymer composite membranes.

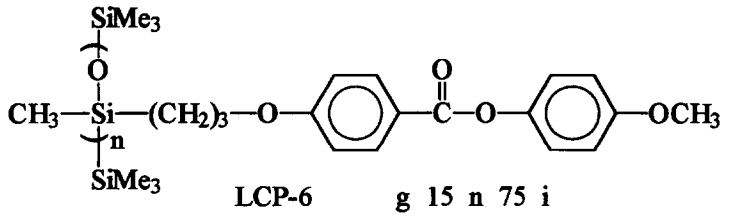


LCP-6 g 15 n 75 i

Fig. 25. Chemical structure and phase transition of the side-chain LC polysiloxane LCP-6.

Paul and collegues[104–108] reported the gas permeation through main-chain LCP membranes. Loth and Euschen[109] investigated the transport behavior of salicylic acid through a liquid-crystalline side-chain elastomer membrane. Candia *et al.*[110] reported the transport behavior of dichloromethane through a smectic side-chain LCP. Finkelmann and co-workers[111–113] have measured the transport behavior of hydrocarbon gases through side-chain LCP elastomer membranes. Our group[114–116] has also studied the gas transport properties of side-chain LCPs/porous polypropylene composite membranes. A representative example of gas permeation through a nematic side-chain LC polysiloxane-based membrane is presented below.

A side-chain LC polysiloxane containing 4-methoxyphenyl-4-allyloxybenzoate side groups (Fig. 25) is used. The polymer exhibits a glassy-to-nematic transition at 15°C and a nematic-yo-isotropic transition at 75°C. During the measurements of gas permeation, two porous polypropylene films were used as supporting layers to give the liquid-crystalline polymer membrane sufficient mechanical strength. This is necessary because the side-chain LCP will become a viscous liquid when it is heated to the liquid-crystalline and isotropic states. The permeation characteristics of the porous polypropylene film were measured, and it showed very high gas permeability with almost no selectivity for all gases used in this study. This result suggests that the permeation properties of the laminated membrane consisting of a side-chain LCP film and two porous polypropylene films were eventually controlled by the side-chain LCP film only.

The permeation results for five gases in the laminated side-chain LCP membrane at various temperatures are summarized in Table 3. For all five gases, the permeability increases as the temperature rises. Figure 26 shows the Arrhenius plots of the permeability $P$ of five gases for the laminated side-chain LCP membrane. A distinct jump of $P$ was observed in the vicinity of the glass transition temperature of the side-chain LCP. For all five gases, the magnitude of $P$ increases approximately five-fold when the temperature increases from 10°C (glassy state) to

Table 3. The temperature dependence of diffusion coefficients ($D$) and solubility coefficients ($S$) for $H_2$, $O_2$, $N_2$, $CH_4$ and $CO_2$ in the laminated side-chain LCP membrane

| $T$ (°C) | $D_{H_2}$ | $D_{O_2}$ | $D_{N_2}$ | $D_{CH_4}$ | $D_{CO_2}$ | $S_{H_2}$ | $S_{O_2}$ | $S_{N_2}$ | $S_{CH_4}$ | $S_{CO_2}$ |
|---|---|---|---|---|---|---|---|---|---|---|
| | $(cm^2/s) \times 10^6$ | | | | | $(cm^3\ (STP)/cm^3\ cmHg) \times 10^4$ | | | | |
| 25 | 4.65 | 0.385 | 0.161 | 0.146 | 0.177 | 4.69 | 4.54 | 2.34 | 4.49 | 61.6 |
| 35 | — | 0.794 | 0.370 | 0.352 | 0.408 | — | 3.89 | 1.91 | 3.35 | 48.5 |
| 45 | — | 1.99 | 1.10 | 0.912 | 1.09 | — | 3.20 | 1.48 | 2.89 | 36.3 |
| 60 | — | — | 3.90 | 3.16 | 3.48 | — | — | 1.21 | 2.35 | 21.3 |

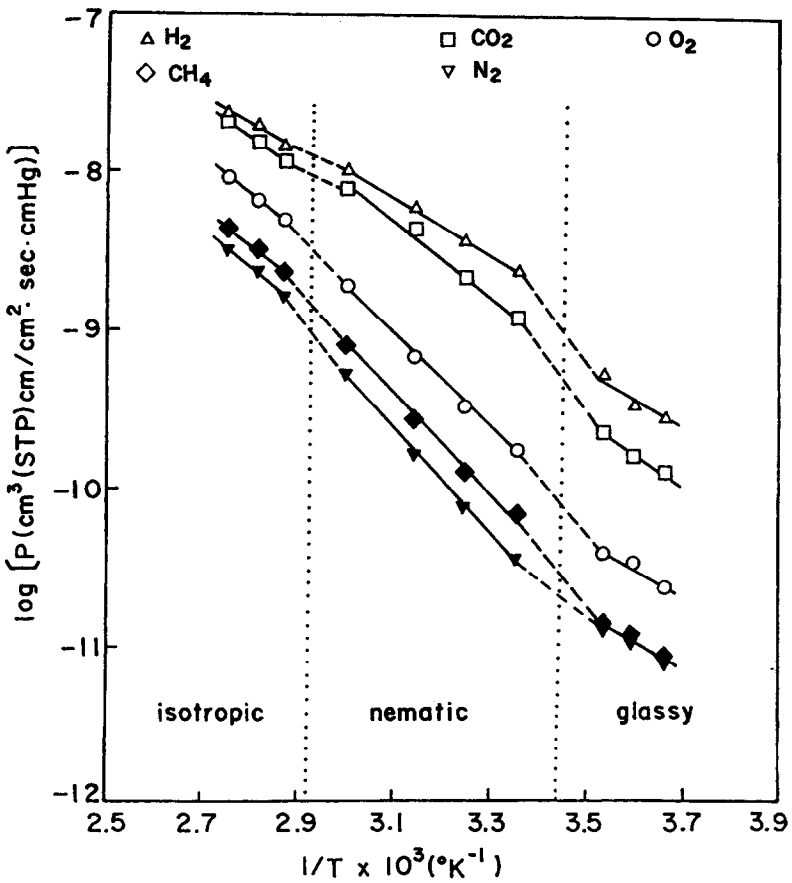


Fig. 26. Arrhenius plots of permeability $P$ in units of $cm^3$ (STP) $cm/cm^2$ s cmHg for various gases in the laminated side-chain liquid-crystalline polysiloxane LCP-6 membrane: $H_2$ (△); $CO_2$ (□); $O_2$ (○); $CH_4$ (◆) and $N_2$ (▼).

25°C (nematic liquid-crystalline state). This result may arise from the high segmental motion in the mesophase of the side-chain LCP. On the other hand, when the temperature increases from the nematic liquid-crystalline state of the side-chain LCP to its isotropic state, no abrupt jump of the permeability was observed. Table 4 summarizes the activation energies for permeation of the side-chain LCP obtained at three different states for five gases. As can be seen from the table, the activation energy for permeation shows the highest value when the side-chain LCP is in the liquid-crystalline state.

Figure 27 shows a plot of the separation factor, $P_{O_2}/P_{N_2}$, versus $P_{O_2}$ for the laminated side-chain LCP membrane. An increase in $P_{O_2}$ on the abscissa corresponds to a rise of the temperature of measurement. In general, the magnitude of the separation factor decreases with increasing permeability. However, the opposite tendency was observed for the laminated side-chain LCP membrane when the temperature rises and the phase changes from its glassy state to its liquid-crystalline state: i.e. the separation factor increased. It seems without

Table 4. The temperature dependence of the permeability coefficients and separation factors, $P_{O_2}/P_{N_2}$ and $P_{CO_2}/P_{CH_4}$, for $H_2$, $O_2$, $N_2$, $CH_4$ and $CO_2$ in the laminated side-chain LCP

| Thermal state of the side-chain LCP | $T$ (°C) | $P_{H_2}$ | $P_{O_2}$ | $P_{N_2}$ | $P_{CH_4}$ | $P_{CO_2}$ | $P_{O_2}/P_{CO_2}$ | |
|---|---|---|---|---|---|---|---|---|
| | | (cm$^3$ (STP) cm/cm$^2$ s cmHg) × $10^{10}$ | | | | | $P_{N_2}$ | $P_{CH_4}$ |
| Glassy | 0 | 2.50 | 0.228 | 0.076 | 0.079 | 1.15 | 3.79 | 14.6 |
| | 5 | 3.07 | 0.330 | 0.110 | 0.102 | 1.46 | 3.00 | 14.3 |
| | 10 | 4.76 | 0.375 | 0.126 | 0.137 | 2.07 | 2.98 | 15.1 |
| Nematic | 25 | 21.8 | 1.75 | 0.380 | 0.655 | 11.1 | 4.60 | 16.9 |
| | 35 | 33.7 | 3.06 | 0.706 | 1.18 | 19.8 | 4.33 | 16.8 |
| | 45 | 55.4 | 6.37 | 1.63 | 2.64 | 39.6 | 3.90 | 15.0 |
| | 60 | 96.5 | 18.6 | 4.95 | 7.42 | 74.2 | 3.75 | 10.0 |
| Isotropic | 75 | 132 | 46.8 | 15.6 | 21.8 | 110 | 3.00 | 5.04 |
| | 82 | 182 | 62.7 | 22.4 | 30.4 | 152 | 2.80 | 5.00 |
| | 90 | 230 | 87.1 | 31.5 | 39.0 | 200 | 2.76 | 5.13 |

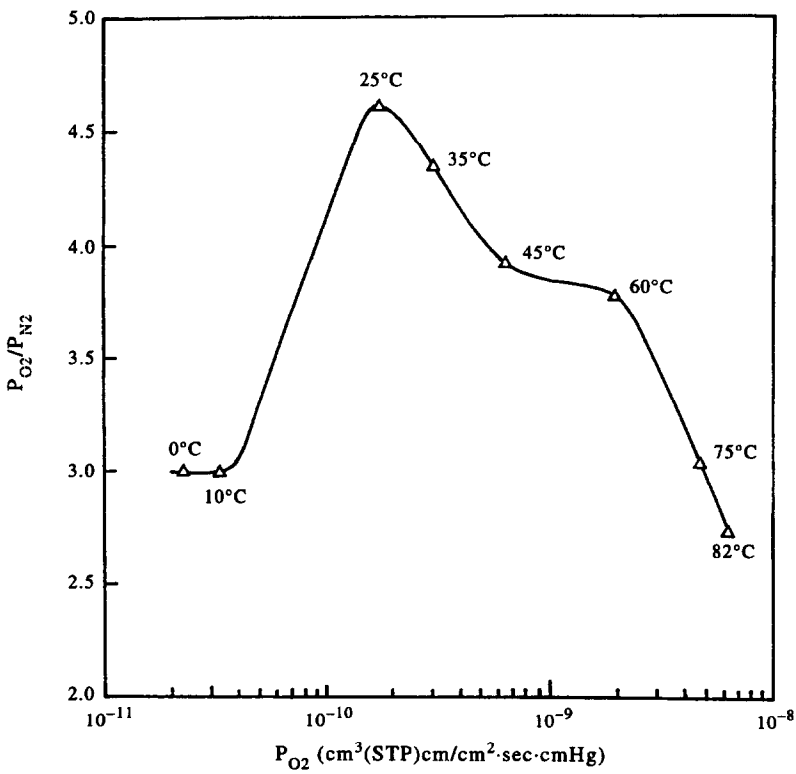


Fig. 27. Plot of the separation factor, $P_{O_2}/P_{N_2}$, versus the permeability of oxygen, $P_{O_2}$ in units of cm$^3$ (STP) cm/cm$^2$ s cmHg, for the laminated side-chain liquid-crystalline polysiloxane LCP-6 membrane and different temperatures as indicated.

Table 5. Activation energies for permeation at three different states of the side-chain LCP

| Gas | $T < T_g$ (glassy) | $T_g < T < T_{NI}$ (nematic) | $T > T_{NI}$ (isotropic) |
|---|---|---|---|
| | $Ep_1$ (kcal/mol) | $Ep_2$ (kcal/mol) | $Ep_3$ (kcal/mol) |
| $H_2$ | 7.43 | 8.35 | 8.00 |
| $O_2$ | 7.48 | 13.43 | 9.91 |
| $N_2$ | 7.83 | 14.50 | 11.77 |
| $CH_4$ | 8.51 | 13.70 | 9.86 |
| $CO_2$ | 8.85 | 10.89 | 9.85 |

doubt that this phenomenon of $P_{O_2}/P_{N_2}$ increase with $P_{O_2}$ is due to the ordered supermolecular arrangement of the side-chain LCP. In detail, according to the structural principle, a side-chain LCP can be roughly separated into two different kinds of microphasic domain: one corresponding to the more or less coiled polymer backbone and the other corresponding to the anisotropically ordered mesogenic side groups. When the temperature is below $T_g$, the segmental motions of the mesogenic side groups are restricted and the frozen liquid-crystalline domains can be considered as barriers for the gases. Therefore, the gas permeation process is predominantly controlled by the amorphous main-chain domains. However, when the temperature rises above $T_g$, the segments of the main chains are free to move and the segmental motions of the side chains become larger. The gases permeate not only through the main-chain domains but also through the ordered mesogenic side-chain domains. The separation factor $P_{O_2}/P_{N_2}$ is mainly controlled by the mesogenic side-chain domains. And its value increases abruptly, because these domains have an ordered supermolecular arrangement.

It is well known that the permeation coefficient can be expressed as a function of the diffusion and the solubility coefficients. According to the time-lag method, the diffusion coefficients for all five gases through the laminated side-chain LCP membrane were estimated. The diffusion and solubility coefficients of the five gases, which were determined by the time-lag method in the nematic liquid-crystalline state of the side-chain LCP, are summarized in Table 5. Among the five gases, the high permeability of hydrogen is mainly attributed to its high diffusivity, while the high permeability of carbon dioxide is mainly attributed to its high solubility.

In order to understand the influence of the liquid-crystalline order on the gas permeation behavior in the laminated side-chain LCP, it is useful to compare the gas transport properties of this membrane with those of some common polymers (see Table 6). All the data listed in Table 6 were obtained at 25°C. At this particular temperature, the side-chain LCP presents a nematic mesophase. Although the polymer backbone of the side-chain LCP is polysiloxane and the side-chain LCP is supposed to have a very high segmental motion in the liquid-crystalline state, the laminated side-chain LCP membrane showed a fairly low permeation coefficient for oxygen. The permeability of oxygen for this membrane was much smaller than those for natural rubber and poly(dimethylsiloxane) and was slightly higher than that for high-density polyethylene. This membrane, however, shows the highest selectivity for oxygen and nitrogen as shown in Table 6. All these results could be due to the ordered supermolecular structure of the liquid-crystalline state exhibited by the side-chain LCP.

In conclusion, the permeation properties in the laminated side-chain LCP were found to depend strongly on the different states of the side-chain LCP. In the liquid-crystalline state of

Table 6. Comparison of gas transport properties at 25°C of the side-chain liquid-crystalline polysiloxane with those of some common polymers

| Polymer* | $P_{O_2}$† | $D_{O_2}$‡ | $S_{O_2}$§ | $P_{O_2}/P_{N_2}$ | $D_{O_2}/D_{N_2}$ | $S_{O_2}/S_{N_2}$ |
|---|---|---|---|---|---|---|
| LCP | 1.75 | 0.385 | 4.54 | 4.60 | 2.39 | 1.93 |
| NR | 23.3 | 1.73 | 13.5 | 2.47 | 1.48 | 1.67 |
| PDMS | 605 | — | — | 2.15 | — | — |
| HPDE | 0.403 | 0.170 | 2.38 | 2.82 | 1.83 | 1.55 |
| LDPE | 2.88 | 0.460 | 6.29 | 2.97 | 1.44 | 2.07 |

*LCP = side-chain liquid-crystalline polysiloxane; NR = natural rubber; PDMS = poly(dimethylsiloxane) (vulcanized, 10% filled); HDPE = polyethylene (density = 0.964); LDPE = polyethylene (density = 0.914).
†Permeability coefficient in $10^{-10}$ $cm^3$ (STP) $cm/cm^2$ s cmHg.
‡Diffusion coefficient in $10^{-6}$ $cm^2/s$.
§Solubility coefficient in $10^{-4}$ $cm^3$ (STP)/$cm^3$.

the side-chain LCP, the separation factors $P_{O_2}/P_{N_2}$ and $P_{CO_2}/P_{CH_4}$ show the highest value, although the gas permeability is not the lowest. This could be due to the ordered supermolecular arrangement of the liquid-crystalline state of the side-chain LCP. The results demonstrate the possibility to achieve a highly permselective membrane simply based on a side-chain LCP.

## 6. THE APPLICATION OF SIDE-CHAIN LCPS AS SOLID POLYMER ELECTROLYTES

Solvent-free polymer electrolytes have attracted considerable attention because of their potential application in high-energy density batteries. The majority of polymer electrolyte systems reported to date have been largely based on poly(oxyethylene), incorporating an alkali metal salt. Only some studies have focused on the complexes formed by alkali metal salts and comb-like polymers containing oligo(oxyethylene) side chains.[118] Interest in these comb-like polymers for the preparation of polymer electrolytes comes from the high segmental mobility of the side chains and the low glass transition temperature exhibited by these polymers, which results in high ionic conductivity of the polymeric electrolytes obtained. Hall *et al.*[119] and Smid and co-workers.[118,120] reported on the conductivity of solid complexes of lithium salts and comb-like polysiloxanes with oligo(oxyethylene) side groups.

Side-chain LCPs with oligo(oxyethylene) spacers have been synthesized widely. The particular interest in this polymer system originates from the possibility of combining the complexing ability of the oligo(oxyethylene) side groups with the supramolecular arrangements as well as the high mobility provided by the mesophases of the LCPs. When this unique polymer system is combined with an inorganic salt it may lead to a complex with high ionic conductivity. Hsieh *et al.*[121,122] first investigated the ionic conductivity of solid polymeric electrolytes based on a side-chain LC polysiloxane (LCP-7). The chemical structure of LCP-7, which contains oligo(oxyethylene) spacers and 6-cyano-2-naphthyl benzyl ether mesogens, is shown in Fig. 28. The LCP-7 shows a $T_g$ at 26°C followed by a liquid-crystalline phase, which undergoes isotropization at 87°C (see Fig. 29).

Addition of lithium salt to the LCP-7 causes a shift in both the glass transition temperature

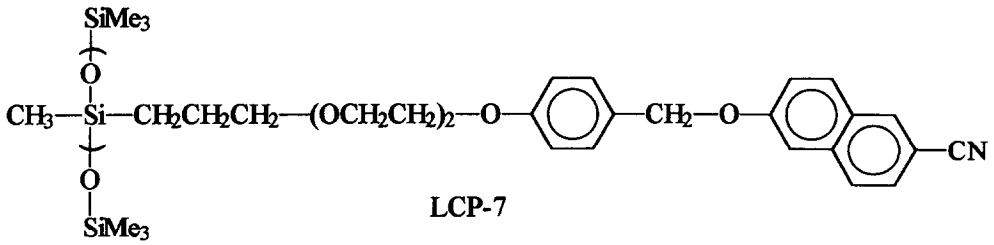


LCP-7

Fig. 28. Chemical structure of side-chain LC polysiloxane LCP-7.

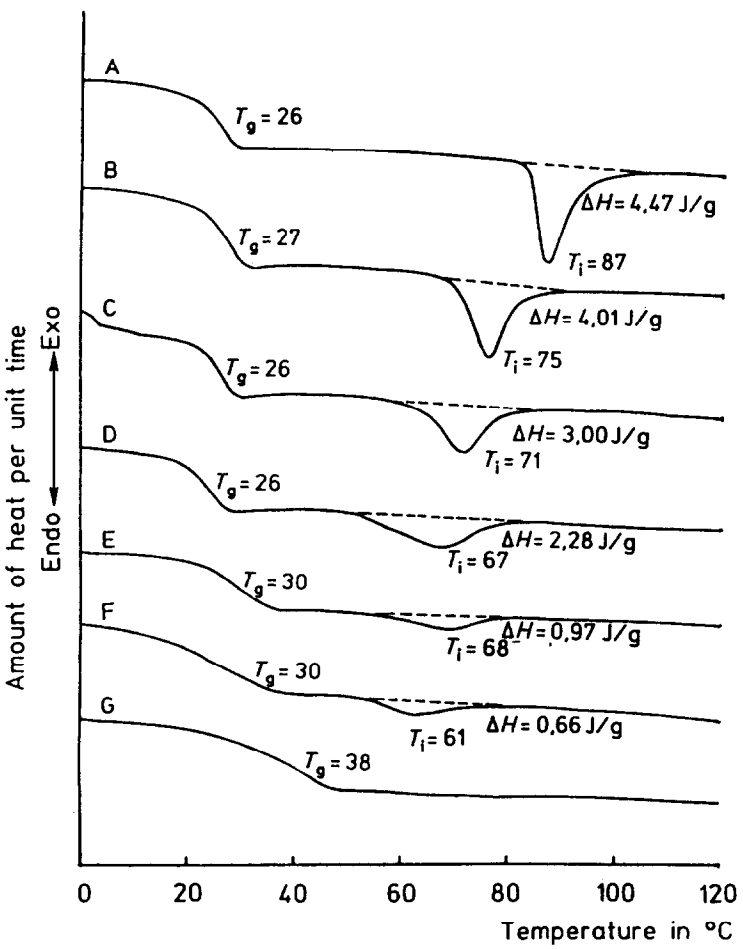


Fig. 29. Normalized DSC traces for pure side-chain liquid-crystalline polysiloxane LCP-7 (A) and $LiSO_3CF_3$/LCP-6 complexes with $LiSO_3CF_3/OCH_2CH_2$ mole ratios of 1/20 (B), 1/10 (C), 1/6 (D), 1/4 (E), 1/2 (F) and 1/1 (G).

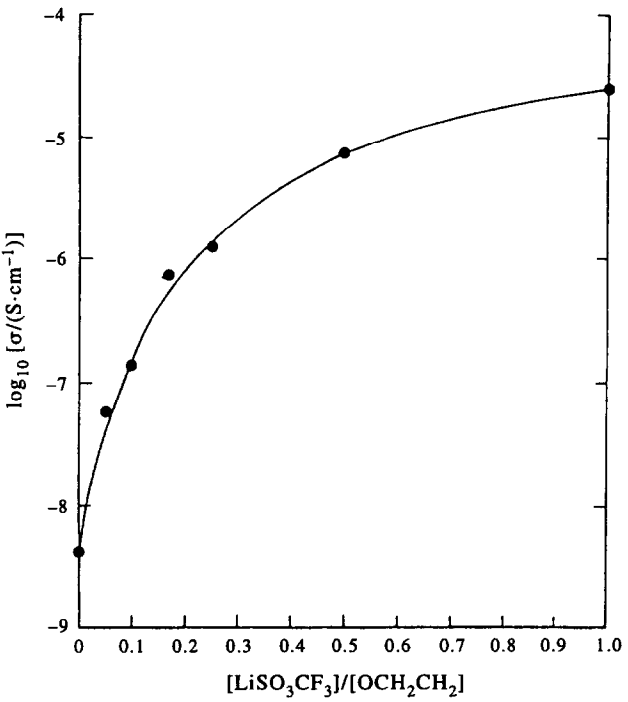


Fig. 30. Logarithm of conductivity $\sigma$ versus $LiSO_3CF_3/OCH_2CH_2$ mole ratio for side-chain liquid-crystalline polysiloxane LCP-7/$LiSO_3CF_3$ complexes at 324 K.

($T_g$) and the isotropization temperature ($T_i$) of the LCP. The glass transition temperatures for LCP-5/$LiSO_3CF_3$ complexes are nearly constant when the mole ratio of $LiSO_3CF_3$ to oxyethylene units ($[Li^+]/[OCH_2CH_2]$) is smaller than 1/6. However, when $[Li^+]/[OCH_2CH_2]$ is higher than 1/6, the $T_g$ of the complexes increases gradually and the transition curves become broader. This suggests that complexation of the salts with the side chains of LCP-7 leads to side-chain stiffening or crosslinking when the salt content is sufficiently large. $T_i$ and the isotropization enthalpy ($\Delta H$) of the complexes decrease with increasing amount of $LiSO_3CF_3$ in the complexes. The reason is that the free liquid-crystalline domain decreases as the salt content increases. Curve G reveals that the free liquid-crystalline domain completely disappears when $[LiSO_3CF_3]/[OCH_2CH_2]$ of a complex is equal to 1.

Figure 30 presents the conductivities at 324 K for the complexes as a function of $[Li^+]/[OCH_2CH_2]$ over the range from 0 to 1. The conductivity increases steadily with increasing the lithium concentration and no maximum peak is observed. This behavior is quite different from that presented by most of the amorphous polymeric electrolyte complexes. The reason could be that the polymer is in a liquid-crystalline state at this temperature and ionic conduction does not proceed via a free-volume mechanism. Therefore, an increase in salt concentration raises the number of charge carriers and increases the conductivity.

The conductivity plotted as logarithm of conductivity versus reciprocal temperature, for the complexes and pure LCP-7, is shown in Fig. 31. The conductivity of pure LCP-5 is basically constant in the temperature range between 237 K and 359 K. This demonstrates

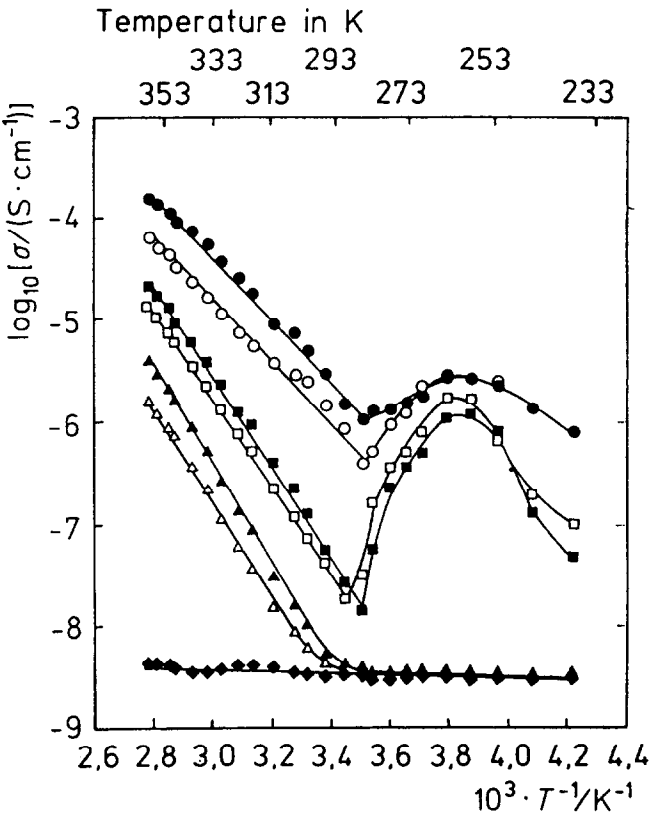


Fig. 31. Logarithm of conductivity $\sigma$ as a function of reciprocal absolute temperature, $1/T$, for side-chain liquid-crystalline polysiloxane LCP-7/$LiSO_3CF_3$ complexes with $LiSO_3CF_3/OCH_2CH_2$ mole ratio of 1/1 (●), 1/2 (○), 1/4 (■), 1/6 (□), 1/10 (▲), 1/20 (△) and 2 (◆).

that impurities have a negligible effect on the conductivities of LCP-5 and the complexes. The maximum conductivity values are $4.8 \times 10^{-6}$ S/cm at ambient temperature and $1.5 \times 10^{-4}$ S/cm at 359 K for the complex with $[Li^+]/[OCH_2CH_2] = 1/1$. The dependence of conductivity on temperature shows a very unusual behavior. Eventually, it can be discussed according to the different phases exhibited by the liquid-crystalline polymer. In the glassy and glass transition states the conductivity increases first with increasing temperature, reaches a maximum at about 263 K and then decreases with increasing temperature for the complexes with $[Li^+]/[OCH_2CH_2] \geq 1/6$.

The possible explanation is that the first increase of conductivity is due to the increase in polymer-chain motion as the temperature increases. When the temperature is further increased to approach the glass transition, the thermal energy becomes roughly comparable to the potential energy barriers to segment rotation and translation. With increasing temperature, the segmental motions of the polymer become more and more large-scale. Therefore, the conductivity decreases during this transition region. In case of complexes with $[Li^+]/[OCH_2CH_2]$ of 1/10 and 1/20, the conductivity is as low as for pure LCP-4 and is constant

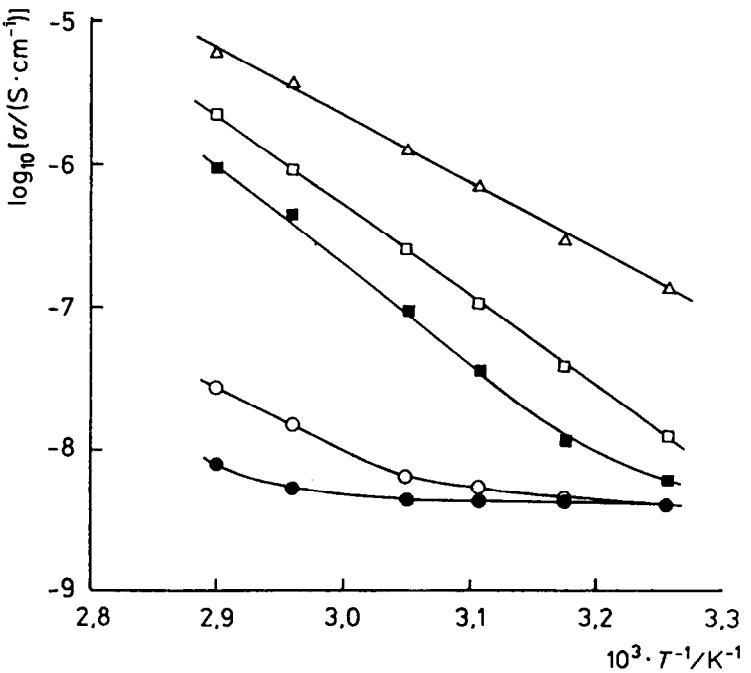


Fig. 32. Logarithm of conductivity $\sigma$ as a function of reciprocal absolute temperature, $1/T$, for complexes of side-chain liquid-crystalline polysiloxane LCP-7 with $LiSO_3CF_3$ (△), $LiClO_4$ (□), $NaClO_4$ (■), LiBr (○) and $KClO_4$ (●) with fixed mole ratio [metal ion]/[$OCH_2CH_2$1 = 1/6.

in the glassy and glass transition states, because the salt content is too low. As the temperature is further increased, the side chains of the polymer begin to rearrange to form the liquid-crystalline structure. In the liquid-crystalline state, the dependence of conductivity on temperature shows Arrhenius-type behavior for all complexes. Both high chain mobility and order in the structure of the polymer cause the conductivity to increase very rapidly.

The conductivities of complexes formed from the LCP-4 with various kinds of alkali metal salts were also studied. Representative plots of the logarithm of conductivity versus reciprocal temperature for complexes with fixed $[M^+]/[OCH_2CH_2] = 1/6$ are shown in Fig. 32 for $LiSO_3CF_3$, $LiClO_4$, LiBr, $NaClO_4$ and $KClO_4$ systems. As can be seen from Fig. 32, the conductivity at a given temperature decreases in the order $LiSO_3CF_3 > LiClO_4 > NaClO_4 >$ LiBr $> KClO_4$. The results depict that the nature of the cation and anion exerts a significant effect on the conductivities of the complexes obtained. It also suggests that $LiSO_3CF_3$ is most effectively ionized by the oxyethylene units of the polymer and thereby a greater number of charge carriers is available in the system.

In conclusion, side-chain LCPs with oligo(oxyethylene) spacers can dissolve metal ions and have been proved to be useful as solid polymer electrolytes. Although the weight fraction of the oxyethylene units in a side-chain LCP is rather low, the conductivity data for the complexes obtained are comparable with those reported for complexes based on other comb-like polymers containing oligo(oxyethylene) side groups. This is due to the

low glass transition temperature and high mobility of the side-chains for the liquid crystal polymers.

The result is rather encouraging. However, more extensive investigations on this field are necessary. In the author's opinion, the conductivity can be improved significantly by on proper molecular design of the side-chain LCPs. For instance, a side-chain LCP with a longer length of oligo(oxethylene) spacers and poly(ethylene oxide) backbone may be a good candidate for the study of solid LC polymeric electrolytes.

## 7. MISCELLANEOUS ASPECTS FOR APPLICATION OF SIDE-CHAIN LCPS

### 7.1. *Application of side-chain LCPs in display technology*

The initial interest in side-chain LCPs can be accounted for by the possibility to create a polymer system combining the unique properties of low-molar-mass liquid crystals and polymers, making it feasible to produce nematic materials for possible use in electro-optical display devices. Results showed that the viscosities of most nematic polymers are too high to be considered as useful replacements for low-molar-mass nematic materials in any fast-switching device. Nevertheless, side-chain LCPs are considered to be useful for some display-related materials, such as polarizers, retardation films and matrices for polymer-dispersed liquid crystals (PDLCs).

Finkelmann[123] first demonstrated that a cholesteric side-chain LCP could be heated above $T_g$, to a temperature at which it was selectively reflective to a desired wavelength of light, and then quenched below $T_g$, thereby locking in both the helical structure of the cholesteric mesophase and the required optical characteristics. This technique makes possible the production of cast films or coatings for use in applications such as optical filters, reflectors or linear polarizers. Recently, Shi and Chen[124] even synthesized some side-LCPs with high birefrigence nematic and chiral nematic mesogens, which can be used as polarizer for display devices.

Super-twisted nematic (STN) liquid crystal displays are currently used widely in the field of liquid crystal displays which require a large-screen display such as, for example, personal computers, word processors and various data terminals. However, since the STN type display via a birefringent effect, coloration such as yellow or blue has been unavoidable. Such a colored-mode display is not only undesirable to users, but also involves the serious drawback of being unable to cope with coloring of a display unit. Shiozaki and Toyooka[125] have reported some side-chain LC copolymers containing cholesteric moieties in the side groups that can be used as a retardation film for STN in order to achieve an achromatic STN liquid crystal display.

Polymer-dispersed liquid crystals (PDLCs) are a new type of light shutter that have been explored in recent years, and are beginning to find applications in switchable windows, large-area displays and projection TVs.[126–129] However, traditional PDLCs made from an isotropic polymeric matrix suffer the disadvantages of low contrast and very narrow viewing angle. Chien *et al.*[130] have demonstrated that using an aligned side-chain LC epoxy as binder for the PDLC can greatly improve the contrast and viewing angle of a PDLC device. The reason is because the refractive indices of both matrix and droplet can be better matched by replacing the isotropic matrix with an anisotropic matrix in a PDLC device.

### 7.2. *Applications of ferroelectric side-chain LCPs in displays, piezoelectric transducers and light modulators*

Ferroelectric liquid crystals have attracted a lot of attention in recent years because of their bistability in display and their short switching time.[131] In 1984 Shibaev *et al.* proved ferroelectricity in an LCP by measuring the temperature-dependent pyroelectric coefficient. Ferroelectric side-chain LCPs show response times in the range of milliseconds by applying a weak electric field.[133] They also show a bistability comparable to that of low-molar-mass LCs. An advantage of such materials in display devices is their better shock resistance and their applicability as flexible display devices.[134]

In 1990, Vallerien *et al.*[135] syntherized a ferroelectic LC elastomer showing piezoelectric behavior. It can be used as a piezoelectric tranducer. Recently, Zentel and collegues[136] synthesized a side-chain LC copolysiloxane with $S_C$* and $S_A$* phases. The polymer shows a huge electroclinic effect in the $S_A$* phase with induced switching angles of up to 45°. The so-called electroclinic effect in this phase gives switching times that are up to 100 times faster (submicrosecond) than in the $S_C$* phase. The high speed of electroclinic switching of the presented polymer could be taken into consideration for the development of light modulators and optoelectronic switches.

### 7.3. *Side-chain LC conducting polymers*

The last two decades has seen the discovery of, and considerable research effort into, the field of electrically conducting organic polymers. A number of polymer systems have been found that, when partially oxidized or reduced (doped), form electronically conducting materials. Polyacetylene is the simplest class of conducting polymers. A high electrical conductivity comparable to that of metal has been reported in $I_2$-doped polyacetylene thin film.[137–139] Recently, Shirakawa and co-workers reported a series of side-chain LC polyacetylenes prepared by Ziegler–Natta and metathesis catalysts (see Fig. 33). To form a liquid-crystalline phase for the conducting polymer is the primary goal for introduction of a mesogenic moiety as a substituted group in polyacetylene. The arrangement of side chains in the liquid-crystalline state may cause an improvement in main-chain conjugation and lead to increased conductivity for the conjugated polymers.

### 7.4. *Applications of side-chain LCPs with metallomesogens as organic ferromagnets*

Molecular design and the construction of organic ferromagnets are the subject of great interest in modern theoretical and organic chemistry. Side-chain LCPs containing

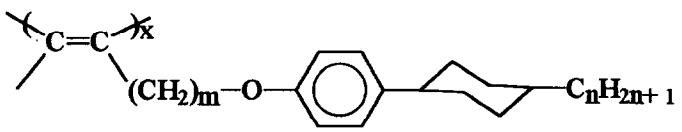


m = 1, 3, 4; n = 0, 3, 5

Fig. 33. Chemical structure of side-chain LC polyacetylenes.

metallomesogens in the side groups have been recently reported.[140–143] Tanaka[144] has demonstrated that this kind of material could be used as organic ferromagnets.

## 8. CONCLUSION AND OUTLOOK

The aim of this paper has been to review recent progress in the applications of side-chain LCPs, especially in the fields of optical data storage, non-linear optics, stationary phases for GC, SFC and HPLC, separation membranes, solid polymer electrolytes and display devices. In the field of optical data storage, both heat-mode and photo-mode recordings have been achieved by side-chain LCPs. Apparently, photo-mode recording based on side-chain LCPs containing photosensitive moieties, such as azobenzenes, spiropyrans and fulgides, shows the bright future for reversible optical data storage.

The side-chain LCPs containing NLO-active moieties in the side groups show second- and third-order NLO properties. However, the SHG and THG values of the poled, amorphous NLO-active polymers, poor poling effficiency and low glass transition are disadvantages for the side-chain LCPs. These disadvantages should be solved for this kind of side-chain LCP in order to compete with other polymeric materials.

Of the side-chain LCP stationary phases, that for gas chromatography is the only one which is commerically available. Recently, more results aimed at using side-chain LCPs for stationary phases of supercritical-fluid chromatography and high-performance liquid chromatography have been reported. In the author's opinion, at least two new areas in side-chain LCP stationary phases are still open for further study. One is the utilization of side-chain LCPs containing chiral moieties for chiral resolution of enantiomers. The other is the utilization of discotic side-chain LCPs as stationary phases.

Only a very few results have appeared in the literatures concerning the application of side-chain LCP as separation membranes and solid polymer electrolytes. The side-chain LCPs basically show abnormal behavior for the transports of drugs, hydrocarbons, gases and metal ions compared with crystalline or amorphous polymers. The detailed transport mechanism of drugs, hydrocarons, common gases and metal ions through side-chain LCP films is presently not very clear. This opens a new field for research. Also, both applications for side-chain LCPs need to be studied more extensively so as to realize commercial products.

Owing to their high viscosities, side-chain LCPs are basically not suitable for replacing low-molar-mass liquid crystals in display applications. However, side-chain LCPs can be used to produce polarizer and retardation films for use in display technology. Both fields deserve great attention since polarizer and retardation films are very important and expensive optical materials in the manufacture of LCD devices.

As we can see from the literature, side-chain LCPs have become most versatile materials in recent years. Through proper molecular design, varieties of new side-chain LCP, such as side-chain LC conducting polymers,[146,146] metallomesogen-containing side-chain LCPs,[140–144] side-chain LC ion–complex polymers,[147–159] side-chain LCPs formed through hydrogen bonding[151–156] and side-chain LCPs containing charge transfer complexes,[157–159] are contiunously becoming available. The author believes that many new potential applications will be found in the near future. Obviously, this review is not able to cover all of them.

Finally, we consider the applications of side-chain LCPs according to their mesomorphic types. Nematic and smectic side-chain LCPs have been widely used for optical data storage, non-linear optics, stationary phases, gas separation membranes, etc. The cholesteric side-chain

LCPs can be used as optical filters, reflectors, linear polarizers and retardation films. Ferroelectic side-chain LCPs can be used for applications such as displays, piezoelectric transducers, pyroelectric detectors and non-linear optics. Both cholesteric and ferroelectric side-chain LCPs are also useful as stationary phases for GC, SFC and HPLC. Most of these applications are based on side-chain LCPs with rod-like mesogens. It is difficult to find reports in the literature concerning the applications of discotic side-chain LCPs. This is a new area, an opening for future studies.

## REFERENCES


1. McArdle, C. B., *Side-Chain Liquid Crystal Polymers*. Blackie press, Glasgow–London, 1989.
2. Shibaev, V. P., Kostromin, S. G., Plate, N. A., Ivanov, S. A., Vetrov, V. Yu. and Yakovlev, I. A., *Polym. Commun.*, 1983, **24,** 364–365.
3. Cole, H. J. and Simon, R., *Polymer*, 1985, **26,** 1801–1806.
4. Eich, M., Wendorf, J. H., Reck, B. and Ringsdorf, H., *Makromol. Chem., Rapid Commun.*, 1987, **8,** 59–63.
5. Eich, M. and Wendorf, J. H., UK Patent 2 193 338, assigned to Rohm GmbH, 1988.
6. Ichimura, K., Suzuki, Y., Seki, T., Kawanishi, Y. and Aoki, K., *Makromol. Chem., Rapid Commun.*, 1989, **10,** 5–8.
7. Angeloni, A. S., Caretti, D., Carlini, C., Chiellini, E., Galli, G., Altomare, A., Solaro, R. and Laus, M., *Liq. Cryst.*, 1989, **4,** 513–527.
8. Weisner, U., Antonietti, M., Boeffel, C. and Spiess, H. W., *Makromol. Chem.*, 1990, **191,** 2133–2149.
9. Sawodny, M., Schmidt, A., Stamm, M., Knoll, W., Urban, C. and Ringsdorf, H., *Polym. Adv. Technol.*, 1991, **2,** 127–136.
10. Angeloni, A. S., Caretti, D., Laus, M., Chiellini, E. and Galli, G., *J. Polym. Sci., Polym. Chem.*, 1991, **29,** 1865–1873.
11. Hvilsted, S., Andruzzi, F. and Ramanujam, P. S., *Opt. Lett.*, 1992, **17,** 1234–1236.
12. Haitjema, H. J., Morgen, G. L. V., Tan, Y. Y. and Challa, G., *Macromolecules*, 1994, **27,** 6201–6206.
13. Anderle, K. and Wendorff, J. H., *Mol. Cryst. Liq. Cryst.*, 1994, **243,** 51–75.
14. Han, Y. K., Kim, D. Y. and Kim, Y. H., *Mol. Cryst. Liq. Cryst.*, 1994, **254,** 445–453.
15. Hvilsted, S., Andruzzi, F., Kulinna, C., Siesler, H. W. and Ramanujam, P. S., *Macromolecules*, 1995, **28,** 2172–2183.
16. Anderle, K., Birenheid, R., Eich, M. and Wendorff, J. H., *Makromol. Chem., Rapid Commun.*, 1989, **10,** 477–483.
17. Ikeda, T., Horiuchi, S., Karanjit, D. B., Kurihara, S. and Tazuke, S., *Macromolecules*, 1990, **23,** 42–48.
18. Ikeda, T., Kurihara, S., Karanjit, D. B. and Tawke, S., *Macromolecules*, 1990, **23,** 3938–3943.
19. Ikeda, T., Hasehawa, S., Saski, T., Miyamoto, T., Lin, M. P. and Tazuke, S., *Makromol. Chem.*, 1991, **192,** 215–221.
20. Anderle, K., Birenheid, R., Werner, M. J. A. and Wendorff, J. H., *Liq. Cryst.*, 1991, **9,** 691–699.
21. Ivanov, S., Yakovlev, I., Kostromin, S., Shibaev, V., Lasker, L., Stumpe, J. and Kreosig, D., *Makromol. Chem., Rapid Commun.*, 1991, **12,** 709–715.
22. Ruhmann, R., Zschuppe, V., Dittmer, M. and Wolff, D., *Makromol. Chem.*, 1992, **193,** 3073–3082.
23. Sasaki, T., Ikeda, T. and Ichimura, K., *Macromolecules*, 1992, **25,** 3807–3811.
24. Ringsdorf, H., Urban, C., Knoll, W. and Sawodny, M., *Makromol. Chem.*, 1992, **193,** 1235–1247.
25. Czapla, S., Ruhman, R., Rubner, J., Zschuppe, V. and Wolff, D., *Makromol. Chem.*, 1993, **194,** 243–250.
26. Sasaki, T., Ikeda, T. and Ichimura, K., *Macromolecules*, 1993, **26,** 151–154.
27. Natasohn, A., Xie, S. and Rochon, P., *Macromolecules*, 1992, **25,** 5531–5532.
28. Natasohn, A., Rochon, P., Gosselin, J. and Xie, S., *Macromolecules*, 1992, **25,** 2268–2273.

29. Rochon, P., Gosselin, J., Natansohn, A. and Xie, S., *Appl. Phys. Lett.*, 1992, **60,** 4–5.
30. Xie, S., Natansohn, A. and Rochon, P., *Chem. Mater.*, 1993, **5,** 403–411.
31. Cebrera, I. and Krongauz, V., *Nature (London)*, 1987, **326,** 582–585.
32. Cebrera, I. and Krongauz, V., *Macromolecules*, 1987, **20,** 2713–2717.
33. Cebrera, I., Krongauz, V. and Ringsdorf, H., *Angew. Chem. Int. Ed. Engl.*, 1987, **26,** 1178–1180.
34. Krongauz, V., *Photochromism Molecules and Systems.* eds. H. Durr and H. Bones-Laurent. Elsevier, Amsterdam, 1990, p. 793.
35. Yitzchaik, S., Ratner, J., Ruchholtz, F. and Krongauz, V., *Liq. Cryst.*, 1990, **8,** 677–686.
36. Zelichenok, A., Buchholtz, F., Yitzchak, S., Ratner, J., Safro, M. and Krongauz, V., *Macromolecules*, 1992, **25,** 3179–3183.
37. Natarajan, L. V., Bunning, T. J., Klei, H. E., Crane, R. L. and Adam, W. W., *Macromolecules*, 1991, **24,** 6554–6556.
38. Natarajan, L. V., Bunning, T. J., Tondigha, U., Patnaik, S., Pachter, R., Crane, R. L. and Adam, W. W., *Chemistry of Functional Dyes*, Vol. 2, ed. Y. Shirota. Mita Press, Kobe, 1993, p. 405.
39. Natarajan, L. V., Tondiglia, V., Bunning, T. J., Crane, R. L. and Adams, W. W., *Adv. Mater. Opt. Electron.*, 1992, **1,** 293–297.
40. Natarajan, L. V., Bunning, T. J. and Kim, S. Y., *Macromolecules*, 1994, **27,** 7248–7253.
41. Prasad, P. N. and Williams, D. J., *Introduction to Nonlinear Optical Effects in Molecules and Polymers.* John Wiley and Sons, Inc., New York, 1991.
42. Meredith, G. R., VanDusen, J. G. and Williams, D. J., *Macromolecules*, 1982, **15,** 1385–1389.
43. Mohlmann, C. R. and Vander Vorst, C. P. J. M., *Side-Chain Liquid Crystal Polymers*, ed. C. B. McArdle. Blackie Press, Glasgow–London, 1989, p. 330.
44. McCulloch, I. A. and Bailey, R. T., *Mol. Cryst. Liq. Cryst.*, 1991, **200,** 157–165.
45. Amano, M., Kaino, T., Yamamoto, F. and Takeuchi, Y., *Mol. Cryst. Liq. Cryst.*, 1990, **182,** 81–90.
46. Koide, N., Ogura, S., Aoyama, Y., Amano, M. and Kaino, T., *Mol. Cryst. Liq. Cryst.*, 1991, **198,** 323–330.
47. Zhao, M., Bautista, M. and Ford, W. T., *Macromolecules*, 1991, **24,** 844–849.
48. Ford, W. T., Bautista, M., Zhao, M., Reeves, R. J. and Powell, R. C., *Mol. Cryst. Liq. Cryst.*, 1991, **198,** 351–356.
49. Wijekoon, W. M. K. P., Zhang, Y., Karna, S. P., Prasad, P. N., Griffin, A. C. and Bhatti, A. M., *J. Opt. Soc. Am.*, 1992, **B9,** 1832–1842.
50. Campbell, D., Dix, L. R. and Rostron, P., *Eur. Polym. J.*, 1993, **29,** 249–253.
51. Bautista, M. O., Duran, R. S. and Ford, W. T., *Macromolecules*, 1993, **26,** 659–667.
52. McL.Smith, D. A. and Coles, H. J., *Liq. Cryst.*, 1993, **14,** 937–946.
53. Dubois, J. C., Le Barny, P., Robin, P., Lemoine, V. and Rajbenbach, H., *Liq. Cryst.*, 1993, **14,** 197–213.
54. Imrie, C. T., Karasz, F. E. and Attard, G. S., *Macromolecules*, 1994, **27,** 1578–1581.
55. Alastair, D., Smith, M. and Coles, H. J., *Polym. Adv. Technol.*, 1994, **6,** 230–236.
56. Abe, J., Hasegawa, M., Matsushima, H., Shirai, Y., Nemoto, N., Nagase, Y. and Takamiya, N., *Macromolecules*, 1995, **28,** 2938–2943.
57. Hsieh, C. J., Wu, S. H., Hsiue, G. H. and Hsu, C. S., *J. Polym. Sci., Polym. Chem.*, 1994, **32,** 1077–1085.
58. Hsiue, G. H., Wu, L. H., Hsiue, C. J. and Jeng, R. J., *Liq. Cryst.*, 1995, **19,** 189–195.
59. Le Barny, P. and Dubois, J. C., *Side Chain Liquid Crystal Polymers*, ed. C. B. McArdle. Blackie Press, Glasgow–London, 1989, p. 130.
60. Shtykov, N. M., Barnik, M. I., Beresnev, L. A. and Blinov, L. M., *Mol. Cryst. Liq. Cryst.*, 1985, **124,** 379–390.
61. Walba, D. M., Ros, M. B., Clark, N. A., Shao, R., Robinson, M. G., Liu, J. Y., Johnson, K. M. and Doroski, D., *J. Am. Chem. Soc.*, 1991, **113,** 5471–5474.
62. Schadt, M., *Liq. Cryst.*, 1993, **14,** 73–104.
63. Schmitt, K., Herr, R. P., Schadt, M., Funfschilling, J., Buchecker, R., Chen, X. H. and Benecke, C., *Liq. Cryst.*, 1993, **14,** 1735–1752.
64. Zental, R., Poths, H., Kremer, F., Schonfeld, A., Jungbaur, D., Twieg, R., Willson, C. G. and Yoon, D., *Polym. Adv. Technol.*, 1992, **3,** 211–217.

65. Schrowsky, G., *Polym. Adv. Technol.*, 1992, **3,** 219–229.
66. Zentel, R., *Polymer*, 1992, **33,** 4040–4046.
67. Brelimer, M., Wiesemann, A., Wischerhoff, E. and Zentel, R., *Mol. Cryst. Liq. Cryst.*, 1994, **254,** 405–416.
68. Wischerhoff, E., Zentel, R., Redmond, M., Mondain-Monval, O. and Coles, H., *Makromol. Chem. Phys.*, 1994, **195,** 1593–1602.
69. Benne, I., Semmler, K. and Finkelmann, H., *Makromol. Chem., Rapid Commun*, 1994, **15,** 295–302.
70. Benne, I., Semmler, K. and Finkelmann, H., *Macromolecules*, 1995, **28,** 1854–1858.
71. Stupp, S. I., Lin, H. C. and Wake, D. R., *Chem. Mater.*, 1992, **4,** 947–953.
72. Broer, D. J., in *Radiation Curing in Polymer Science and Technology*, Vol. 3, eds. J. P. Fouasser and J. F. Rabek. Elsevier, London–New York, 1993, p. 393.
73. Janini, G. M., *Adv. Chromatogr.*, 1979, **17,** 231–277.
74. Witkiewicz, Z., *J. Chromatogr.*, 1982, **251,** 311–337.
75. Finkelmann, H., Laub, R. J., Roberts, W. L. and Smith, C. A., in *Polynuclear Aromatic Hydrocarbons: Physical and Biological Chemistry*, eds. M. Cooke, A. J. Dennis and G. L. Fisher. Battele Press, Columbus, OH, 1982, p. 275.
76. Janini, G. M., Laub, R. J. and Purnell, J. H., in *Side Chain Liquid Crystal Polymers*, ed. C. B. McArdle. Blackie Press, Glasgow–London, 1989, p. 395.
77. Witkiewicz, Z., *J. Chromatogr.*, 1989, **466,** 37–87.
78. Witkiewicz, Z. and Mazur, J., *LC-GC*, 1990, **8,** 224–236.
79. Naikwadi, K. P., Jadhav, A. L., Rokushika, S., Hatano, H. and Ohshima, M., *Makromol. Chem.*, 1986, **187,** 1407–1414.
80. Jadhav, A. L., Naikwadi, K. P., Rokushika, S., Hatano, H. and Ohshima, M., *J. High Resolut. Chromatogr., Chromatogr. Commun.*, 1987, **10,** 77–81.
81. Rokushika, S., Naikwadi, K. P., Jadhav, A. L. and Hatano, H., *J. High Resolut. Chromatogr., Chromatogr. Commun.*, 1985, **8,** 480–484.
82. Rokushika, S., Naikwadi, K. P., Jadhav, A. L. and Hatano, H., *Chromatographia*, 1986, **22,** 209–212.
83. Chang, H.-C. K., Markides, K. E., Bradshaw, J. S. and Lee, M. L., *J. Chromatogr. Sci.*, 1988, **26,** 280–289.
84. Kithinji, J. P., Raynor, M. W., Egia, B., Davies, I. L., Bartle, K. D. and Clifford, A. A., *J. High Resolut. Chromatogr.*, 1990, **13,** 27–33.
85. Klein, B. H. and Springer, J., *J. Liq. Chromatogr.*, 1991, **14,** 1519–1538.
86. Klein, B. H. and Springer, J., *J. Liq. Chromatogr.*, 1991, **14,** 1539–1559.
87. Pesek, J. J. and Cash, T., *Chromatographia*, 1989, **27,** 559–564.
88. Pesek, J. J., Vidensek, M. A. and Miller, M., *J. Chromatogr.*, 1991, **556,** 373–381.
89. Pesek, J. J., Lu, Y., Siouffi, A. and Grandperrin, F., *Chromatographia*, 1991, **31,** 147–151.
90. Pesek, J. J. and Williamsen, E. J., *Trends Anal. Chem.*, 1992, **11,** 259–266.
91. Hanson, M. and Unger, K. K., *Trends Anal. Chem.*, 1992, **11,** 368–373.
92. Saito, Y., Jinno, K., Pesek, J. J., Chen, Y. L., Luehr, G., Archer, J., Fetzer, J. C. and Biggs, W. R., *Chromatographia*, 1993, **38,** 295–303.
93. Menster, M. K., Bombick, D. D., Flora, D. B., Bunning, T. J., Klei, H. E. and Crane, R. L., *Polym. Prepr.*, 1992, **33,** 1150–1151.
94. Lin, J. L. and Hsu, C. S., *Polym. J.*, 1993, **25,** 153–167.
95. Percec, V. and Rodenhouse, R., *Macromolecules*, 1989, **22,** 4408–4412.
96. Wen, J. S., Hsiue, G. H. and Hsu, C. S., *Makromol. Chem., Rapid Commun.*, 1990, **11,** 151–157.
97. Hsiue, G. H., Wen, J. S. and Hsu, C. S., *Makromol. Chem.*, 1991, **192,** 2243–2254.
98. Fu, R., Jing, P., Gu, J., Huang, Z. and Chen, Y., *Anal. Chem.*, 1993, **65,** 2141–2144.
99. Zhou, W., Fu, R., Dai, R., Huang, Z. and Chen, Y., *J. Chromatogr.*, 1994, **659,** 477–480.
100. Kajiyama, K., Nagata, T., Maemura, E. and Takayanagi, M., *Chem. Lett.*, 1979, 679–682.
101. Washizu, S., Terada, I., Kajiyama, T. and Takayanagi, M., *Polym. J.*, 1984, **4,** 307–316.
102. Kajiyaina, T., Washizu, S. and Takayanagi, M., *J. Appl. Polym. Sci.*, 1984, **29,** 3955–3964.
103. Kajiyama, T., Washizu, S., Kumano, A., Terada, I. and Takayanagi, M., *J. Appl. Polym. Sci., Appl. Polym. Symp.*, 1985, **41,** 327–346.

104. Chlou, J. S. and Paul, D. R., *J. Polym. Sci., Polym. Phys.*, 1987, **25,** 1699–1707.
105. Weinkauf, D. H. and Paul, D. R., *J. Polym. Sci., Polym. Phys.*, 1991, **29,** 329–340.
106. Weinkauf, D. H. and Paul, D. R., *J. Polym. Sci., Polym. Phys.*, 1992, **30,** 817–849.
107. Weinkauf, D. H. and Paul, D. R., *J. Polym. Sci., Polym. Phys.*, 1992, **30,** 837–849.
108. Weinkauf, D. H., Kim, H. D. and Paul, D. R., *Macromolecules*, 1992, **25,** 788–796.
109. Loth, H. and Euschen, A., *Makromol. Chem., Rapid Commun.*, 1988, **9,** 35–38.
110. de Candia, F., Capodanno, V., Renzulli, A. and Vitoria, V., *J. Appl. Polym. Sci.*, 1991, **42,** 2959–2963.
111. Modler, H., Reincke, H. and Finkelmann, H., *Polym. Mater. Sci. Eng.*, 1989, **61,** 497–501.
112. Modler, H. and Finkelmann, H., *Ber. Bunsenges. Phys. Chem.*, 1990, **94,** 836–856.
113. Reinecke, H. and Finkelmann, H., *Makromol. Chem.*, 1992, **193,** 2945–2960.
114. Chen, D. S., Hsiue, G. H. and Hsu, C. S., *Makromol. Chem.*, 1991, **192,** 2021–2029.
115. Chen, D. S., Hsiue, G. H. and Hsu, C. S., *Makromol. Chem.*, 1992, **193,** 1469–1479.
116. Chen, D. S. and Hsiue, G. H., *Makromol. Chem.*, 1993, **194,** 2025–2033.
117. Watanabe, M. and Ogata, M., *Br. Polym. J.*, 1988, **20,** 181–192.
118. Khan, I. M., Yuan, Y., Fish, D., Wu, E. and Smid, J., *Macromolecules*, 1988, **21,** 2684–2689.
119. Hall, P. G., Davis, G. R., McIntyre, J. E., Ward, I. M., Bannister, D. J. and Le Broeq, K. M. F., *Polym. Commun.*, 1986, **27,** 98–100.
120. Fish, D., Khan, I. M., Wu, E. and Smid, J., *Br. Polym. J.*, 1988, **20,** 281–288.
121. Hsieh, C. J., Hsu, C. S. and Hsiue, G. H., *J. Polym. Sci., Polym. Chem.*, 1990, **28,** 425–435.
122. Hsieh, C. J., Hsiue, G. H. and Hsu, C. S., *Makromol. Chem.*, 1990, **191,** 2195–2230.
123. Finkelmann, H., *Phil. Trans. Roy. Soc. Lond.*, 1983, **A309,** 105–114.
124. Shi, H. and Chen, S. H., *Macromolecules*, 1993, **26,** 5840–5843.
125. Shimaki, I. and Toyooka, T., US Patent 5 193 020, 1993.
126. Doane, J. W., Vaz, N. P., Wu, B. G. and Zumer, S., *Appl. Phys. Lett.*, 1986, **48,** 269–271.
127. Drazak, P. S., *J. Appl. Phys.*, 1986, **60,** 2142–2148.
128. Wu, B. G., West, J. L. and Doane, J. W., *J. Appl. Phys.*, 1987, **62,** 3925–3931.
129. West, J. L., *Mol. Cryst. Liq. Cryst*, 1988, **157,** 427–441.
130. Chien, L. C., Lin, C., Fredley, D. S. and McCargar, J. W., *Macromolecules*, 1992, **25,** 133–137.
131. Clark, N. A. and Lagerwall, S. T., *Appl. Phys. Lett.*, 1980, **36,** 899–901.
132. Shibaev, V. P., Kozlovsky, M. V., Beresneu, L. A., Blinov, L. M. and Plate, N. A., *Polym. Bull.*, 1984, **12,** 299–301.
133. Scherowsky, G., Schliwa, A., Springer, J., Kuhnpast, K. and Trapp, W., *Liq. Cryst.*, 1989, **5,** 1281–1295.
134. Yuasa, K., Uchida, S., Sekiya, T., Hashimoto K. and Kawasaki, K., in *Proceedings of Third International Conference on Ferroelectric Liquid Crystals*, Boulder, CO, 1991, pp. 24–28.
135. Vallerien, S. U., Kremer, F., Fischer, E. W., Kapitza, H., Zentel, R. and Poths, H., *Makromol. Chem., Rapid Commun.*, 1990, **11,** 593–598.
136. Poths, H., Andersson, G., Skarp, K. and Zentel, R., *Adv. Mater.*, 1992, **4,** 792–794.
137. Naarmann, H. and Thephilon, N., *Synth. Met.*, 1987, **22,** 1–8.
138. Akagi, K., Suezaki, M., Shirakawa, H., Kyotani, H., Shimomura, M. and Tanabe, Y., *Synth. Met.*, 1989, **28,** D1–D18.
139. Tsukamoto, T., Takahashi, A. and Kawasaki, K., *Jpn J. Appl. Phys.*, 1990, **29,** 125–130.
140. Hanabusa, K., Suzuki, T., Koyama, T., Shirai, H. and Kurose, A., *Polym. J.*, 1990, **22,** 183–186.
141. Hanabusa, K., Suzuki, T., Koywna, T. and Shiral, H., *Makromol. Chem.*, 1992, **193,** 2149–2161.
142. Hanabusa, K., Isogai, T., Koyama, T. and Shirai, H., *Makromol. Chem.*, 1993, **194,** 197–210.
143. Tanaka, H., *Eur. Polym. J.*, 1993, **29,** 1525–1530.
144. Tanaka, H., *Kobunshi*, 1994, **43,** 734–735.
145. Oh, S. Y., Ezaki, R., Akagi, K. and Shirakawa, H., *J. Polym. Sci., Polym. Chem.*, 1993, **31,** 2977–2985.
146. Oh, S. Y., Akagi, K., Shirakawa, H. and Araya, K., *Macromolecules*, 1993, **26,** 6203–6206.
147. Ujiie, S. and Iimura, K., *Macromolecules*, 1992, **25,** 3174–3178.
148. Branday, F. A. and Bawin, C. G., *Polym. Prepr.*, 1993, **34 (1),** 186–187.
149. Roche, P. and Zhao, Y., *Macromolecules*, 1995, **28,** 2819–2824.

150. Nieuwkerk, A. C., Marcelies, A. T. M. and Subholter, E. J. R., *Macromolecules*, 1995, **28,** 4986–4990.
151. Kato, T. and Frechet, J. M. J., *Macromolecules*, 1989, **22,** 3818–3819.
152. Kato, T. and Frechet, J. M. J., *Macromolecules*, 1990, **23,** 360.
153. Kato, T. and Frechet, J. M. J., *J. Am. Chem. Soc.*, 1989, **111,** 8533–8534.
154. Kato, T., Hideyuki, K., Urya, T., Fujishima, A. and Frechet, J. M. J., *Macromolecules*, 1992, **25,** 6836–8641.
155. Kumar, U., Kato, T. and Frechet, J. M. J., *J. Am. Chem. Soc.*, 1992, **114,** 6630–6639.
156. Kato, T., Frechet, J. M. J., Wilson, P. G., Saito, T., Uryr, T., Fujishima, A., Jin, C. and Kaneuchi, F., *Chem. Mater.*, 1993, **5,** 1094–1100.
157. Imfie, C. T., Karasz, F. and Attard, G. S., *Liq. Cryst.*, 1991, **9,** 47–57.
158. Schleeh, T., Imrie, C. T., Rice, D. M., Karasz, F. E. and Attard, G. S., *J. Polym. Sci., Polym. Chem.*, 1993, **31,** 1859–1869.
159. Kosaka, Y., Kato, T. and Uryu, T., *Macromolecules*, 1994, **27,** 2658–2663